

# 1

## Introduction to Mass Spectrometry, a Tutorial

Wilfried M.A. Niessen and David Falck

### 1.1

#### Introduction

In the past 30 years, mass spectrometry (MS) has undergone a spectacular development, in terms of both its technological innovation and its extent of application. On-line liquid chromatography–mass spectrometry (LC–MS) has become a routine analytical tool, important in many application areas. The introduction of electrospray ionization (ESI) and matrix-assisted laser desorption/ionization (MALDI) has enabled the MS analysis of highly polar and large molecules, including biomacromolecules. MS is based on the generation of gas-phase analyte ions, the separation of these ions according to their mass-to-charge ratio ( $m/z$ ), and the detection of these ions. A wide variety of ionization techniques are available to generate analyte ions (Section 1.3). Mass analysis can be performed by six types of mass analyzers (Section 1.4), although quite frequently tandem mass spectrometers, featuring the combination of two mass analyzers, are used (Section 1.5). The data acquired by MS allow quantitative analysis of target analytes, determination of the molecular mass/weight, and/or structure elucidation or sequence determination of (unknown) analytes (Section 1.6).

This chapter provides a general introduction to MS, mainly from a functional point of view. Next to basic understanding of operating principles of ionization techniques and mass analyzers, the focus is on data interpretation and analytical strategies required in the study of biomolecular interactions using MS.

### 1.2

#### Figures of Merit

#### 1.2.1

##### Introduction

An MS experiment typically consists of five steps: (i) sample introduction, (ii) analyte ionization, (iii) mass analysis, (iv) ion detection, and (v) data processing and

interpretation of the results. Sample introduction may involve individual samples or may follow (on-line) chromatographic separation. Mass analysis and ion detection require a high vacuum (pressure  $\leq 10^{-5}$  mbar). Analyte ionization may take place either in high vacuum or at atmospheric pressure. In the latter case, a vacuum interface is required to transfer ions from the atmospheric-pressure ionization (API) source into the high-vacuum mass analyzer region.

In its basic operation with on-line chromatography or other forms of continuous sample introduction, the mass spectrometer continuously acquires mass spectra, that is, the instrument is operated in the full-spectrum (or full-scan) mode. This means that a three-dimensional data array is acquired, defined by three axes: time,  $m/z$ , and ion intensity (counts). This data array can be visualized in different ways (Figure 1.1). In the *total-ion chromatogram* (TIC), the sum of the ion counts in the individual mass spectra are plotted as a function of time. A *mass spectrum* represents a slice of the data array of the ion counts as a function of  $m/z$  at a particular time point. Summed, averaged, and/or background subtracted mass spectra can be generated. Mass spectra may be searched against libraries, when available, to assist in compound identification. In an *extracted-ion chromatogram* (XIC), the counts for the ion with a selected  $m/z$  are plotted as a function of time. The  $m/z$  selection window may be adapted to the resolution of the mass spectrometer. In instruments providing unit-mass resolution, the selection window in most cases is  $\pm 0.5$   $m/z$  units (u), whereas with high-resolution mass spectrometry (HRMS, see below) selection windows as small as  $\pm 10$  mu can be used (narrow-window XIC). In a *base-peak chromatogram* (BPC), the ion count recorded for the most abundant ion in each spectrum is plotted as a function of time. BPCs are especially useful for peak searching in chromatograms with relatively high chemical background. More advanced tools of data processing are discussed in Section 1.6.1.

Three figures of merit are relevant: mass spectrometric resolution, mass accuracy, and the acquisition speed, that is, the time needed to acquire one spectrum (or one data point in a chromatogram).

### 1.2.2

#### Resolution

Despite the fact that mass spectrometrists readily discuss (and boast) on the resolution of their instruments, it seems that there is no unambiguous definition available. The IUPAC (International Union of Pure and Applied Chemistry) recommendations [1] and ASMS (American Society for Mass Spectrometry) guidelines [2] are different in that respect [3, 4]. Most people in the MS community define *resolution* as  $m/\Delta m$ , where  $m$  is the mass of the ion (and obviously should be read as  $m/z$ ) and  $\Delta m$  is either the peak width (mostly measured at full-width half-maximum, FWHM) or the spacing between two equal-intensity peaks with a valley of, for instance, 10% [1]. The FWHM definition is generally used with all instruments, except sector instruments where the valley definition is used. The *resolving power* is defined as the ability to distinguish two ions with a small difference in  $m/z$ . However, resolving power has also been defined as  $m/\Delta m$  and the

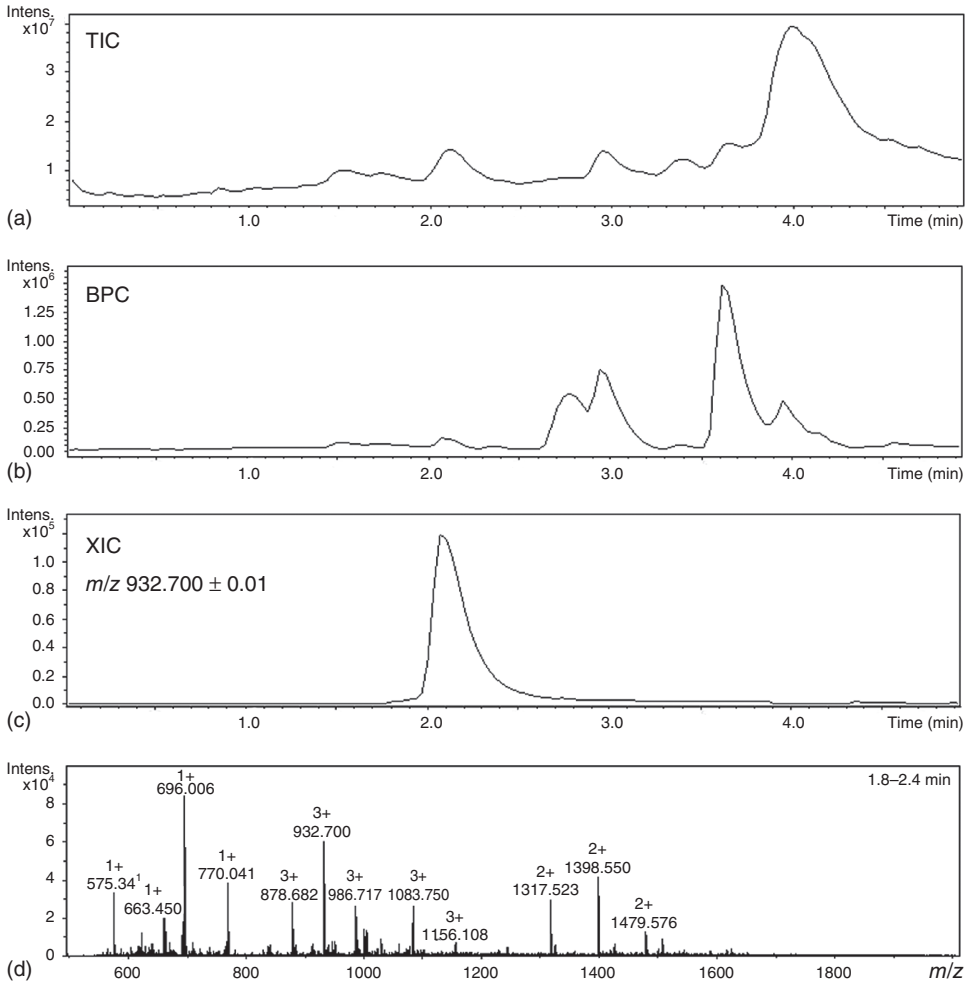


**Figure 1.1** Visualization of the three-dimensional data array acquired in a full-spectrum MS experiment. (a) Total-ion chromatogram (TIC), (b) base-peak chromatogram (BPC), (c) extracted-ion chromatogram (XIC), and (d) mass spectrum. Data for an

*N*-glycopeptide from the LC–MS analysis of a tryptic digest of a commercial immunoglobulin G (IgG) standard, analyzed using a Dionex Ultimate 3000 nano-LC coupled via ESI to a Bruker Maxis Impact Q-TOF MS in the laboratory of one of the authors (D. Falck).

resolution as the inverse of resolving power [3]. The IUPAC definition is used throughout this text.

In a simple and straightforward way, mass analyzers can be classified as either unit-mass-resolution or high-resolution instruments (see Table 1.1). For unit-mass-resolution instruments such as quadrupoles and ion traps, calculation of the resolution as  $m/\Delta m$  is not very useful, as the FWHM is virtually constant over the entire mass range.

**Table 1.1** Characteristics and features of different mass analyzers.

Analyzer	Resolution <sup>a)</sup>	Mass accuracy	Full-spectrum performance <sup>b)</sup>	Selected-ion performance <sup>b)</sup>	Pressure (mbar)
Quadrupole	Unit-mass	±0.1	+	++	<10 <sup>-5</sup>
Ion-trap	Unit-mass	±0.1	++	+	10 <sup>-5</sup>
Time-of-flight	≤70 000	<3 ppm	++	–	<10 <sup>-7</sup>
Orbitrap	≤140 000	<1 ppm	++	–	<10 <sup>-9</sup>
FT-ICR	≤400 000	<1 ppm	++	–	<10 <sup>-9</sup>
Sector	≤60 000	<3 ppm	+	++	<10 <sup>-7</sup>

a) Resolution based on FWHM definition, except for sector (5% valley definition).

b) ++, instrument highly suitable for this operation; +, instrument less suitable for this operation; and –, instrument not suitable for this operation (post-acquisition XIC possible).

### 1.2.3

#### Mass Accuracy

In MS, the mass of a molecule or the  $m/z$  of an ion is generally expressed as a monoisotopic mass (molecular mass) or  $m/z$ , referring to the masses of the most abundant natural isotopes of the elements present in the ion or molecule. In chemistry, the average mass or molecular weight is used, based on the average atomic masses of the elements present in the molecule. The *exact mass* (or better  $m/z$ ) of an ion is its calculated mass, that is, its theoretical mass. In this respect, the charge state of the ion is relevant, because the electron mass (0.55 mDa) may not be negligible. The *accurate mass* (or better  $m/z$ ) of an ion is its experimentally determined mass, measured with an appropriate degree of accuracy and precision. The accurate mass is the experimental approximation of the exact mass. The *nominal mass* (or better  $m/z$ ) is the mass of a molecule or an ion calculated using integer values for the masses of the most abundant isotopes of the elements present in the molecule or ion. The *mass defect* is the difference between the exact mass and the nominal mass of ion or molecule [1, 5].

The achievable mass accuracy in practice depends on the resolution of the mass analyzer and the quality and stability of the calibration of the  $m/z$  axis. An instrument providing unit-mass resolution generally allows  $m/z$  determination for single-charge ions with an accuracy of ±0.1 u (nominal mass determination). In HRMS, the *mass accuracy* is generally expressed either as an absolute mass error (accurate mass – exact mass, in mu) or as a relative error (in ppm), calculated from

$$\frac{(\text{accurate mass} - \text{exact mass})}{(\text{exact mass})} \times 10^6$$

In HRMS of small molecules, the error in  $m/z$  determination will typically be in the third decimal place (accurate mass determination).

From the accurate  $m/z$  of an ion, one can use software tools to calculate its possible elemental compositions. The number of hits from such a calculation

obviously depends on the  $m/z$  value, the number of elements considered, and the mass accuracy achieved [6]. The number of hits may also be reduced by taking an accurately measured isotope pattern of the ion into consideration [7, 8]. For a given ion with  $m/z$   $M$ , the relative abundances of the ions with  $m/z$   $M+1$ ,  $M+2$ , and  $M+3$  reveal the presence (or absence) and even the number of specific elements, for example, Cl, Br, and S from the  $M+2$  ion. For small molecules (<1 kDa), the maximum number of carbon atoms in the molecule can be estimated by dividing the relative abundance (in percent) of the  $M+1$  peak by 1.1. Ultra-HRMS instruments have additional possibilities to derive elemental composition, as they can even separate the contributions of different atoms to the  $M+2$  isotope peak. This is illustrated for an unknown compound with  $C_{13}H_{24}N_3O_6S_2$  in an onion bulb in Figure 1.2 (see also [9]).

As discussed in Section 1.6.6, mass accuracy also has a distinct influence on the ease and quality of protein identification from peptide-mass fingerprints or peptide-sequence analysis approaches.

#### 1.2.4

##### General Data Acquisition in MS

The general mode of data acquisition of a mass spectrometer is the full-spectrum (or full-scan) mode. In this mode, mass spectra are continuously acquired between

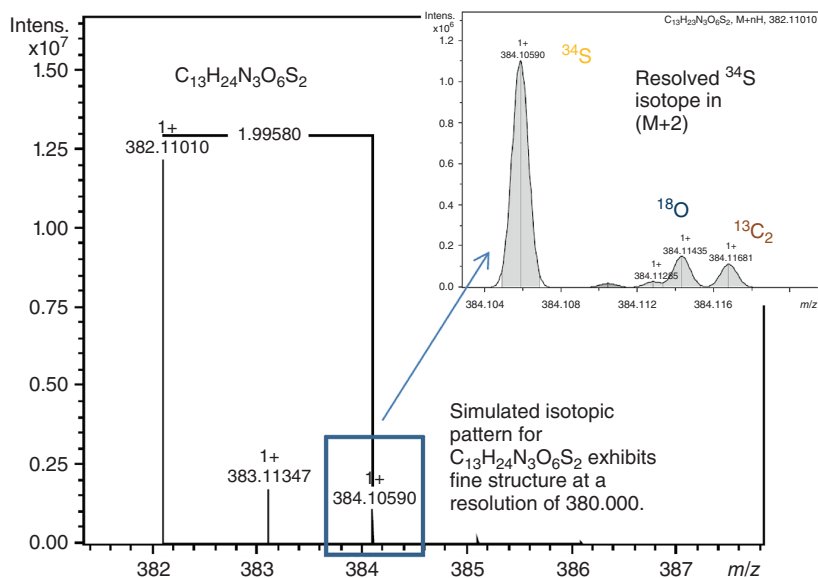


**Figure 1.2** Demonstration of high-resolution mass spectrometry. Simulated isotopic pattern for an unknown compound with  $C_{13}H_{24}N_3O_6S_2$  in an onion bulb with isotopic fine structure exhibited at

a resolution of 380 000. (Reprinted with permission from Prof. Kazuki Saito (RIKEN Plant Science Center, Yokohama, Japan) and Bruker Daltonics Application Note # LC-MS 85, ©2013, Bruker Daltonics, 1822187.)

a low  $m/z$  and a high  $m/z$  within a preset period of time (mostly  $\leq 1$  s). Obviously, the information content of the spectrum depends on (i) the selected ionization technique, (ii) the resolution of the instrument, and (iii) data system parameters. The mass spectra are acquired in continuous or profile mode, that is, with a number of data points per  $m/z$  value. For unit-mass-resolution instruments,  $\sim 10$  data points per  $m/z$  suffice, whereas in HRMS far more data points per  $m/z$  are required to provide the appropriate resolution and mass accuracy. Either the profile data are saved by the data system, eventually after some data reduction such as apodization to reduce the data file size (see, e.g., [10]), or centroiding is performed, where only a weighted average of the mass peak is saved [4]. The latter greatly reduces the data file size. Post-acquisition data processing tools may require either profile or centroid data.

Some mass analyzers (see Table 1.1) can also acquire data in the selected-ion mode, which means that the mass analyzer is programmed to select a particular  $m/z$  for transmission to the detector during a preset period (the so-called dwell time, typically 5–200 ms) and to subsequently jump to other preselected  $m/z$  values; after monitoring all selected  $m/z$  values, the same function is repeated for some time, for example, during (part of) the chromatographic run time. Thus, compared to the full-spectrum mode, the MS has a longer measurement time of the selected ion, and thus provides enhanced signal-to-noise ratio (S/N). The data can be displayed in terms of XICs. This acquisition mode is especially applied in targeted quantitative analysis. With HRMS instruments not capable of a selected-ion mode, improved S/N and targeted quantitative analysis can be achieved post-acquisition in narrow-window XICs (see Section 1.2.1).

For a proper understanding of the possibilities and limitations of MS, one should be aware of the fact that a mass spectrometer can generally perform only one experiment at a time. However, various experiments can be performed consecutively. Functions may be defined to perform various experiments repeatedly. As outlined in Section 1.6.1, decisions for the next experiment may be based on the data acquired in the previous experiment (data-dependent acquisition, DDA). The time required for individual MS experiments very much depends on the type of instrument used (and its purchase date). Because of the huge progress in faster electronics, modern instruments can perform faster than older instruments.

### 1.3

#### Analyte Ionization

##### 1.3.1

##### Introduction

More than 50 analyte ionization techniques are available for MS. An ionization technique has to generate gas-phase analyte ions, either in (high) vacuum or transferable from atmospheric pressure into high vacuum, to enable

subsequent mass analysis. The various ionization techniques can be classified in different ways.

Analyte ionization techniques can be classified based on the physical state of the analyte molecules: (i) gas or vapor, (ii) liquid or in solution, or (iii) solid or dry on a target. Traditional ionization techniques such as electron ionization (EI) and chemical ionization (CI) are examples of gas-phase ionization techniques, and are thus frequently used in on-line gas chromatography–mass spectrometry (GC–MS). ESI, which is extensively used in on-line LC–MS and peptide and protein analysis, is a liquid-phase ionization technique, whereas MALDI and desorption electrospray ionization (DESI) are examples of solid-phase or surface ionization techniques. Gas-phase ionization requires either gas-phase samples or evaporation of the analytes before ionization. Surface ionization techniques are frequently so-called energy-sudden techniques [11], in which intense localized energy is applied to the sample, for example, by means of a laser pulse, to simultaneously ionize and transfer the ion from the solid phase to the gas phase. In liquid-phase ionization, the sample solution, for example, the LC (liquid chromatography) mobile phase, is nebulized into small droplets, from which gas-phase analyte ions are generated, for example, in ESI.

A second classification is based on the amount of internal energy that is put into the molecule on generation of the ion. In a hard ionization technique such as EI, typically a few electron volts internal energy is transferred to the molecular ion,  $M^{+\bullet}$ . This internal energy results in rapid in-source compound-specific fragmentation. The mixture of intact molecular ions and fragment ions is subsequently mass-analyzed. In a soft-ionization technique, hardly any internal energy is transferred to the ion during the ionization process. Often, a protonated or deprotonated molecule,  $[M+H]^+$  or  $[M-H]^-$ , is generated and no in-source fragmentation occurs. Some ionization techniques allow some control over the amount of energy deposited in the ion on its formation.

A third classification is based on the type of primary ions generated in the ionization process. The molecular ion,  $M^{+\bullet}$ , generated in EI, is an odd-electron ion ( $OE^{+\bullet}$ ), whereas the protonated or deprotonated molecule,  $[M+H]^+$  or  $[M-H]^-$ , generated in ESI or MALDI, are either positive- or negative-charge even-electron ions ( $EE^+$  or  $EE^-$ ). In this context, the nitrogen rule is important, which states that a molecule, a  $M^{+\bullet}$ , or any other  $OE^{+\bullet}$  with an odd mass or  $m/z$  should contain an odd number of N atoms, whereas a (single-charge)  $EE^+$  with an odd  $m/z$  contains an even number of N atoms. For a known elemental composition, the nitrogen rule allows discriminating between  $OE^{+\bullet}$  and  $EE^+$  ions.

Another useful tool is the double-bond equivalent (DBE), “degree of unsaturation,” or “ring double bond” (RDB) parameter. The DBE can be calculated from the elemental composition of the molecule of ion, using the equation:

$$DBE = 1 + C - \frac{1}{2}(H + F + Cl + Br + I) + \frac{1}{2}(N + P)$$

The DBE is a measure of the number of unsaturations in the molecule, that is, the number of rings and/or double bonds. DBE is an integer number for a molecule or an  $OE^{+\bullet}$  and a number ending at 0.5 for an  $EE^+$  ion. For molecules with P and S

atoms, the DBE does not consider the double bonds in, for instance, a phosphate  $((\text{RO})_3\text{P}=\text{O})$ , a phosphorothioate  $((\text{RO})_3\text{P}=\text{S})$ , a sulfoxide  $(\text{S}=\text{O})$ , or a sulfone  $(\text{SO}_2)$  as a double bond.

### 1.3.2

#### Electrospray Ionization

In ESI, a solution, for example, the mobile phase from an LC column, is nebulized into an API source as a result of a strong electric field, eventually assisted by  $\text{N}_2$  as a nebulizing gas and heating. Small, highly charged droplets (1–10  $\mu\text{m}$ ) are generated. Gas-phase ions are generated in the process of droplet evaporation and field-induced electrohydrodynamic disintegration of the droplets [12]. The gas-vapor mixture ( $\text{N}_2$  and mobile-phase solvents) with analyte ions is sampled from the ion source into the vacuum interface. Desolvation and collisional cooling of the ions occur when they move through the vacuum interface toward the high-vacuum mass analyzer [13]. In most cases, either  $[\text{M}+\text{H}]^+$  or  $[\text{M}-\text{H}]^-$  is generated, depending on the operating polarity, but other adduct ions such as  $[\text{M}+\text{Na}]^+$  or  $[\text{M}+\text{CH}_3\text{COO}]^-$  may be generated as well (or instead).

In terms of instrumentation, significant improvements in the performance of ESI interfaces have been achieved. In the ion source itself, the orthogonal rather than axial positioning of the electrospray needle is important to reduce contamination of the ion-sampling orifice. In the vacuum interface, ion transmission has been improved by the use of continuously more advanced RF-only (radiofrequency) ion focusing and transport devices, that is, next to RF-only quadrupoles (see also Section 1.4.2), hexapoles, and octapoles and also the implementation of ion funnels [14] and traveling-wave stacked-ring ion guides [15]. Whereas in most analytical applications of ESI-MS low pressure is pursued in the vacuum interface, the preservation of protein complexes in native-MS is best achieved at somewhat higher pressures in this region [16]; valves have been implemented to allow pressure adjustments in native-MS experiments.

The ionization mechanism of ESI is not fully understood [12, 17, 18]. The two prevailing models are the *charge-residue model* of Dole [19] and the *ion-evaporation model* of Iribarne and Thomson [20, 21]. Both models assume that analyte molecules are present in solution as preformed ions, which can, for instance, be achieved by choosing an appropriate *pH* of the solution or the mobile phase. According to the *charge-residue model*, the sequence of solvent evaporation and electrohydrodynamic droplet disintegration proceeds until the microdroplets contain only one preformed analyte ion per droplet. By evaporation of the solvent, the preformed analyte ion is released to the gas phase. According to the *ion-evaporation model*, gas-phase ions are generated from the highly charged microdroplets, because the local field strength is high enough for preformed ions to be emitted into the gas phase. Although the two models are to some extent complementary, the relative importance of either mechanism in the actual ion production of a particular analyte is difficult to decide. Smith and Light-Wahl [18] discussed whether the preservation of noncovalent associates of

proteins and drugs in ESI is reasonable within the context of proposed ionization mechanisms for ESI. They argue that the stripping of noncovalently associated solvent molecules from the highly desolvated multiprotonated molecules can be achieved without influencing other noncovalent drug–protein associations. They suggested that the initial highly charged droplets in the 1- $\mu\text{m}$ -I.D. range repeatedly disintegrate to generate nanodroplets in the 10-nm-I.D. range. The latter further shrink by evaporation to yield the ions detected in MS.

Given the importance of droplet evaporation during ESI, the generation of smaller droplets is more favorable in term of sensitivity and the ability to preserve noncovalent molecular associates. This can be achieved by using nanoelectrospray ionization (nESI), where the analyte is sprayed, for example, from a gold-coated fused-silica capillary with a tip diameter of 1–5  $\mu\text{m}$  rather than from the 100 to 150- $\mu\text{m}$  tips that are used in conventional (pneumatically assisted) ESI. Flow rates as low as 20  $\text{nl min}^{-1}$  can be nebulized [22]. Thus, gentler operating conditions (temperature, gas flows, needle voltage) can be achieved. nESI is extensively used in the analysis of biomacromolecules, that is, in native MS, where intact protein complexes are studied [16], as well as in combination with nano-LC for proteomics studies [23, 24]. Integrated chip-based nano-LC-nESI devices have also been developed [25].

ESI enables the soft ionization of highly labile and nonvolatile compounds such as (oligo)nucleotides, (oligo)saccharides, peptides, and proteins without significant fragmentation. In the analysis of biomacromolecules, an ion envelope of multiple-charge ions,  $[M+nH]^{n+}$  or  $[M-nH]^{n-}$ , is generated (see Figure 1.3), from which the molecular weight of the molecule can be accurately calculated (better than 0.01%) using software procedures (see Section 1.6.5).

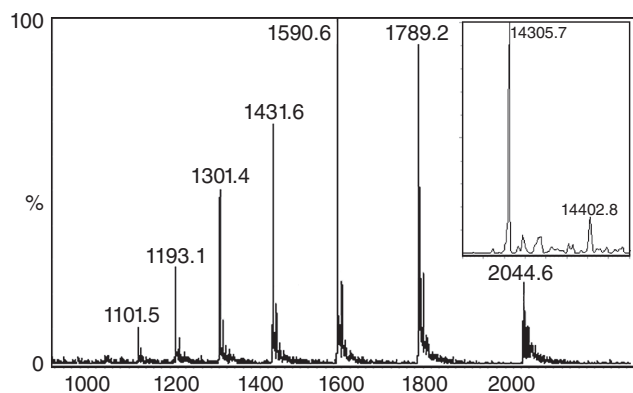


**Figure 1.3** Electrospray ionization mass spectrum of hen egg lysozyme, showing an ion envelope of multiple-charge ions  $[M+nH]^{n+}$ . Inset: Deconvoluted or transformed spectrum. (Reprinted after

modification with permission of Prof. Alison Ashcroft (Biomolecular Mass Spectrometry Group at University of Leeds, UK) from <http://www.personal.leeds.ac.uk/~fbsmaspe/tutorial.html>.)

## 1.3.3

**Matrix-Assisted Laser Desorption Ionization**

Next to ESI, MALDI is the most important ionization technique in the analysis of biomacromolecules. MALDI was introduced in 1988 [26, 27]. In a typical MALDI experiment, 0.3–1  $\mu\text{l}$  of an aqueous analyte solution is mixed with 0.5–1  $\mu\text{l}$  of a  $\sim 5$  mM solution of an appropriate matrix, for example, sinapinic acid, 2,5-dihydroxybenzoic acid, or  $\alpha$ -cyano-4-hydroxycinnamic acid, in 50% aqueous acetonitrile containing 0.1% trifluoroacetic acid, and then deposited onto a metal target. On drying, cocrystallization of matrix and analyte molecules takes place. When these crystals are laser-bombarded with photons that fit the absorption maximum of the matrix, for example, with 337 nm from a  $\text{N}_2$  laser for the matrices mentioned, gas-phase analyte ions are generated in the selvedge, which can be mass-analyzed by a time-of-flight mass spectrometer (TOF-MS) [28, 29]. Unlike ESI, where ion envelopes of multiple-charge ions are generated, mostly single-charge protonated molecules  $[\text{M}+\text{H}]^+$  are generated in MALDI-MS, together with less abundant  $[\text{M}+2\text{H}]^{2+}$  and  $[2\text{M}+\text{H}]^+$  ions.

MALDI-TOF-MS is widely applied especially in the analysis of proteins, peptides, and oligosaccharides [28–30]. It is used in bottom-up protein identification using peptide-map fingerprinting approaches (Section 1.6.6). Currently, MALDI-MS plays an important role in two emerging application areas of MS: imaging MS [31] and identification of bacteria and microbial fingerprinting [32].

Surface-enhanced laser desorption ionization (SELDI-TOF-MS) is a variation of MALDI. Instead of an inert metal target, a modified target is applied to achieve biochemical affinity with the analyte molecules [33]. In SELDI, the protein mixture is spotted onto the surface with a specific (bio)chemical functionality, for example, cation- or anion-exchange materials, hydrophobic materials, or materials with immobilized metal affinity, lectin, or even protein or antibody affinity. Specific proteins in the mixture bind to the surface, while others can be removed by washing. Thus, on-target biomolecular interactions are used as part of the measurement strategy. The specific binding to the SELDI target acts as a sample pretreatment and/or analyte isolation step. After washing, a matrix is applied and the experiments proceeds as in MALDI-TOF-MS [33]. SELDI-TOF-MS is currently extensively used for clinical diagnostics and in clinical biomarker discovery studies.

## 1.3.4

**Other Ionization Methods**

Next to EI, ESI, and MALDI, already discussed, there is a wide variety of other analyte ionization techniques. In coupling of LC and MS, atmospheric-pressure chemical ionization (APCI) is an important alternative to ESI. In APCI, the LC mobile phase is nebulized by pneumatic nebulization. The aerosol is evaporated in a heated zone of the interface probe, enabling soft desolvation of analyte molecules. The gas-phase CI is initiated by a corona discharge needle, which

ionizes the mobile-phase constituents, which in turn ionize the analyte molecules by gas-phase ion–molecule reactions. Again, mainly  $[M+H]^+$  or  $[M-H]^-$  ions are generated with little internal energy. APCI is generally limited to molecules with masses below 1 kDa, but can ionize somewhat less polar analytes than ESI.

In the past decade, a large number of, sometimes closely related, atmospheric-pressure surface ionization techniques have been introduced [34]. DESI may serve as an example. If a high-velocity spray of charged microdroplets from a (pneumatically assisted) electrospray needle is directed at a surface, mounted in front of the ion-sampling orifice of an API source, gas-phase ions from the surface material or surface constituents can be observed by MS [35]. In this way, analytes may be studied at surfaces without extensive sample pretreatment, for example, to analyze drugs of abuse in tablets. The introduction of such surface ionization techniques also opens possibilities to perform chemical imaging of surfaces such as thin-layer chromatography plates and tissue sections [36].

In paperspray ionization (PSI), biomolecules are ionized from a paper tip emerged with nonpolar solvents such as hexane or toluene, placed in the electric field close to the ion-sampling orifice of an API source [37]. Although the polar biomolecules are largely insoluble in these solvents,  $[M+H]^+$ ,  $[M+Na]^+$ , or  $[M-H]^-$  ions are observed. Meanwhile, the technique has found several applications, including the analysis of noncovalent protein complexes [38].

### 1.3.5

#### Solvent and Sample Compatibility Issues

In both ESI and MALDI, the ionization efficiency of a particular analyte may be influenced by the solvent composition, but also by (coeluting, when LC separation is applied) sample constituents. Either ionization enhancement or ionization suppression may take place. If the effect is due to sample constituents, it is mostly called a *matrix effect* [39]. If not dealt with properly, matrix effects can have highly detrimental effects on accuracy and precision in routine quantitative analysis. However, matrix effects, especially severe ionization suppression, may also have distinct influence on the analyte response of constituents of complex mixtures during qualitative analysis. High salt concentrations, nonvolatile salts, surface-active components, for example, phospholipids in blood-related samples, and proteins are known for their matrix effects in small-molecule quantitative bioanalysis. Nonvolatile compounds, be it sample constituents or solvent additives, may result in ionization suppression, in reducing response or S/N by extensive formation of background ions at every  $m/z$ , formation of alkali metal ion adducts or  $H^+/Na^+$ -exchange products, and/or ion source contamination.

Optimization of the sample composition and/or mobile-phase composition, if LC separation is involved, is important to achieve the best response and selectivity in MS. Systematic studies on the influence of additives on ESI performance have been reported [40, 41] and give an initial idea on which additives

can be applied and which ones should be avoided. With respect to buffers, preferably only volatile buffer constituents are permitted, that is, ammonium salts of formic, acetic, or carbonic acid. Borate, citrate, and phosphate buffers, frequently applied in LC, but also many of the buffer systems such as TRIS and HEPES, frequently used in biochemistry, are not compatible with ESI-MS. The same holds for components frequently applied to help solubilizing proteins, that is, detergents such as TWEEN and sodium dodecylsulfate (SDS) and chaotropic agents such as urea and guanidine·HCl. This limits the applicability of ESI-MS in the analysis of proteins that are difficult to solubilize, for example, membrane proteins. Although MALDI-MS is considered less impacted by the presence of such additives on the target, various reports indicate that severe ionization suppression may occur in MALDI-MS as well [42, 43]. This is especially important as MALDI-MS approaches are less likely to be preceded by a separation step.

High concentrations of proteins should not be introduced in ESI-MS. This means that on analysis of undigested blood-related samples (whole blood, plasma, serum), care must be taken. In most applications of intact protein analysis by MS, either the concentrations applied are relatively low or the amount introduced is low due to the use of nESI flow rates.

## 1.4

### Mass Analyzer Building Blocks

#### 1.4.1

##### Introduction

In this section, the different mass analyzers are briefly discussed, with special attention on their possibilities and limitations. A summarizing overview on the available mass analyzers is provided in Table 1.1. Most of them may be used as stand-alone systems, when equipped with an ion source of choice, a detection system, and a data system. Alternatively, they may be combined into tandem MS (MS–MS) systems (see Section 1.5).

Any discussion on mass analyzers should perhaps start with introducing the sector instrument, which is historically at the basis of all MS developments. Ions with mass  $m$  and  $z$  elementary charges  $e$  are accelerated with a voltage  $V$  into a magnetic field  $B$  with a path with a radius of curvature  $r$ . One can derive the equation  $m/z = B^2 r^2 e / 2V$ , which indicates that the separation of ions with different  $m/z$  can be achieved in three different ways: by variation of the radius of curvature ions with different  $m/z$  are separated in space, while by variation of either  $B$  or  $V$  ions of different  $m/z$  are separated in time, that is, they can be detected one after another by a single-point detector at a fixed position behind a slit [44]. Better performance of the sector instrument in terms of mass resolution is achieved by combining the magnetic sector with an electrostatic analyzer, resulting in a double-focusing instrument, which provides

high resolution and accurate mass determination. Until the mid-1990s, the sector instrument was the instrument of choice for HRMS and accurate mass determination. Since then, it has been rapidly replaced by alternatives that are less expensive and much easier to operate, especially in combination with API sources.

#### 1.4.2

##### Quadrupole Mass Analyzer

A quadrupole mass analyzer or mass filter consists of four hyperbolic- or circular-shaped rods that are accurately positioned parallel in a radial array (Figure 1.4a). Opposite rods are charged by either a positive or a negative direct-current (DC) potential, at which an alternating-current (AC) potential in the radiofrequency region (megahertz, thus indicated as RF) is superimposed. At a given DC/RF combination, only the ions of a particular  $m/z$  show a stable trajectory and are transmitted to the detector, while ions with unstable trajectories do not pass the mass filter, because the amplitude of their oscillation becomes infinite. Thus, the quadrupole acts as a variable band pass filter [46]. By changing DC and RF in time, usually at a fixed ratio, ions with different  $m/z$  values can be transmitted to the detector one after another.

The quadrupole mass filter can be operated in four modes. (i) It can be applied in full-spectrum mode by scanning DC and RF in a fixed ratio, providing generally unit-mass resolution and nominal monoisotopic mass determination with great ease of operation, versatility, fast scanning, and limited costs. Scan speeds as high as  $10\,000\text{ u s}^{-1}$  can be achieved. (ii) Alternatively, it can be applied in selected-ion monitoring (SIM) mode, dwelling on selected  $m/z$  values, and capable of rapidly switching (within  $\leq 5\text{ ms}$ ) between different  $m/z$  values. In SIM mode, significantly improved  $S/N$  can be achieved, making the SIM mode of a quadrupole ideal for routine targeted quantitative analysis. (iii) In RF-only mode, the quadrupole can be used as an ion-transport and focusing device. As such, RF-only quadrupole and related hexapole or octapole devices have been used in vacuum interfaces of API-MS systems and as collision cells and/or ion-transport devices in MS-MS instruments (Section 1.5.2). (iv) Finally, a quadrupole mass analyzer can be applied as a linear ion trap (LIT), providing similar features as the conventional three-dimensional ion traps (see Section 1.4.3) [47–49]. The majority of mass spectrometers installed and used are based on quadrupole mass analyzer technology.

#### 1.4.3

##### Ion-Trap Mass Analyzer

A typical (three-dimensional quadrupole) ion trap consists of a cylindrical ring electrode and two end-cap electrodes (Figure 1.4b) [50, 51]. The end-cap electrodes contain holes for the introduction of ions from an external ion source and for the ejection of ions toward an external detector. A He bath gas ( $\sim 1\text{ mbar}$ ) is

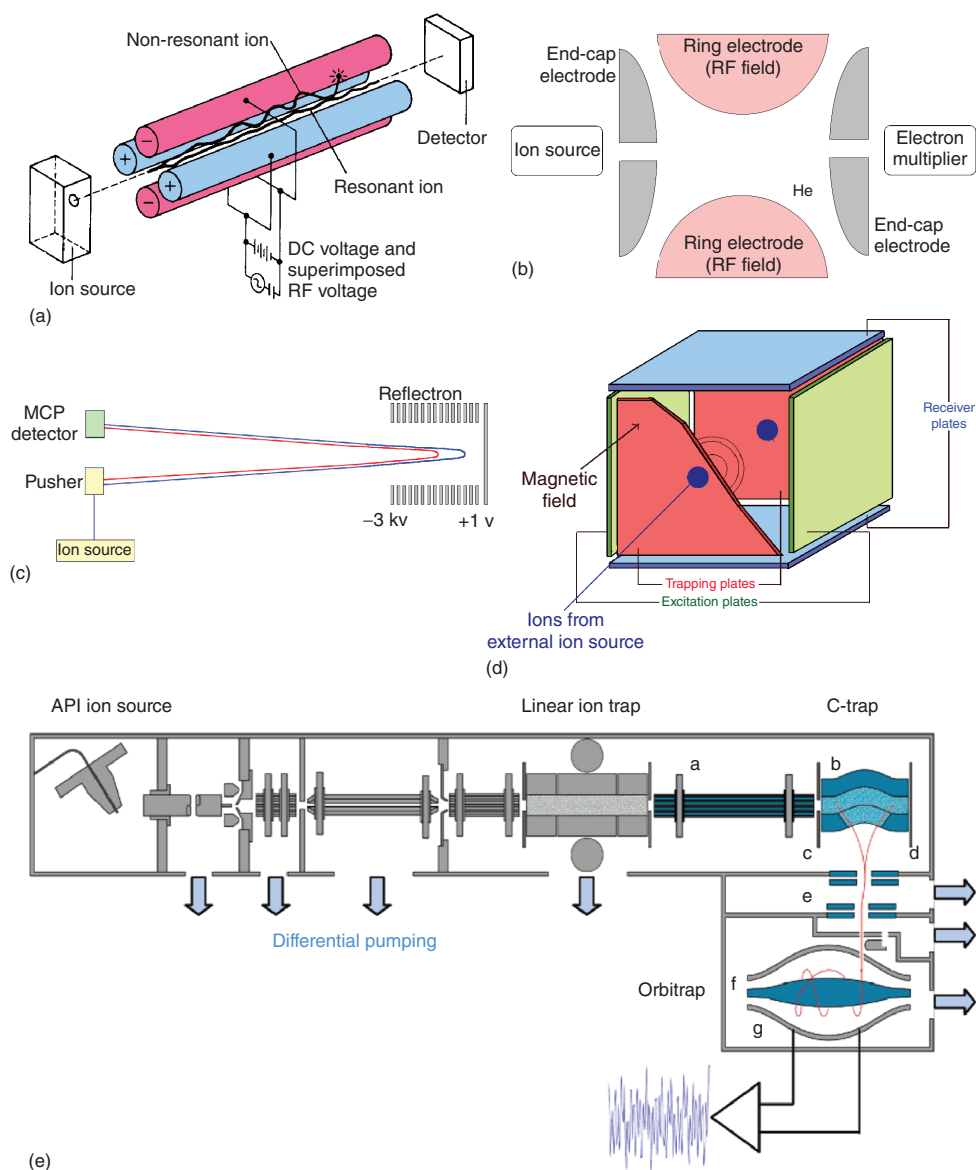


**Figure 1.4** Schematic diagrams of various mass analyzers, with (a) quadrupole mass analyzer, (b) ion-trap mass analyzer, (c) orthogonal-acceleration reflectron time-of-flight mass analyzer, (d) cell of a Fourier-transform ion-cyclotron resonance mass

spectrometer, and (e) linear-ion-trap-orbitrap hybrid mass spectrometer. (All diagrams from the authors' collection, except (e) which is reprinted with permission from Ref. [45]. © 2006, American Chemical Society.)

used to stabilize the ion trajectories in the trap. The basic mass analysis process consists of two steps, performed consecutively in time: (i) injection of ions by means of an ion injection pulse of variable duration and storage of the ions in the trap by application of an appropriate low RF voltage to the ring electrode and (ii) ramping the RF voltage at the ring electrode to consecutively eject ions with different  $m/z$  values from the trap toward the external detector (resonant ion ejection) [50, 51]. As too high numbers of ions in the ion trap adversely influences mass resolution and accuracy due to space-charge effects, the number of ions that can be stored in the trap is limited. Software control of the duration of the ion injection pulse from the external ion source with the ion current at the time has been developed [51]. Ion ejection and subsequent detection can be achieved with unit-mass resolution, or at enhanced resolution by slowing down the scan rate.

A typical feature of an ion-trap MS is its excellent full-spectrum sensitivity, resulting from the accumulation of ions in the first step. The system can be operated in SIM mode, but the gain achieved is far less than in a quadrupole. The resolution achieved depends on the scan speed and the age of the instrument. Older ion traps provide peak widths (FWHM) of 0.2 u at a scan speed of  $\sim 300 \text{ u s}^{-1}$ , unit-mass resolution (FWHM  $\sim 0.7 \text{ u}$ ) at  $5500 \text{ u s}^{-1}$ , and degraded resolution (FWHM of 3.0 u at  $55\,000 \text{ u s}^{-1}$ ), whereas more recently introduced systems provide better resolution at higher scan speeds, for example, FWHM of 0.1 u at  $4600 \text{ u s}^{-1}$  and of 0.58 u at  $52\,000 \text{ u s}^{-1}$ . A FWHM of 0.1 u enables almost baseline resolution for [4+] ions.

More recently, linear two-dimensional ion traps (LIT) were introduced as an alternative to three-dimensional ion traps [47–49]. Because a LIT is less prone to space-charging effects, a higher number of ions can be accumulated, and enhanced sensitivity ( $\sim 60\times$ ) can be achieved. LITs are extensively used in hybrid MS–MS instruments (see Section 1.5.6), but stand-alone versions of a LIT have been introduced as well, thus competing with the three-dimensional ion traps. A dual-pressure two-stage LIT has been reported as well: the first high-pressure ion trap serves to capture, select, and fragment ions, whereas the second low-pressure ion trap is used to perform fast scanning of product ions, eventually at enhanced resolution [52].

#### 1.4.4

##### Time-of-Flight Mass Analyzer

A time-of-flight (TOF) instrument consists of a pulsed ion source, an accelerating grid, a field-free flight tube, and a detector [53, 54]. The flight time  $t$  needed by the ions with a particular  $m/z$ , accelerated by a potential  $V$ , to reach the detector placed at a distance  $d$ , can be calculated from  $t = d \times \sqrt{\{m/(2zeV)\}}$ . Pulsing of the ion source is required to avoid the simultaneous arrival of ions of different  $m/z$  at the detector. In MALDI-TOF-MS experiments, the pulse rate of the source is directly related to the pulse rate of the laser (typically  $<1 \text{ kHz}$ ). One of the benefits is, in principle, the unlimited mass range of the TOF-MS. When combined with continuous ion sources, such as ESI, much higher pulse frequencies are

applied (20–50 kHz). The spectra from multiple pulses are accumulated, providing enhanced spectrum quality by averaging random noise. In LC–MS, spectra acquisition rates up to 50 spectra per second have been reported.

The resolution of a TOF-MS is limited by the speed of the detection and acquisition electronics, which nowadays is hardly a limiting factor, and by the initial ion kinetic energy spread of the ions. Delayed extraction [55], orthogonal acceleration [53], and especially the use of a reflectron [53, 56] are powerful tools to reduce the deteriorating effect of the ion kinetic energy spread on the resolution. The reflectron, consisting of a series of equally spaced grid or ring electrodes connected to a resistive network, creates a homogenous or curved retarding field that acts like an ion mirror. Assume that two ions with the same  $m/z$  but slightly different kinetic energy enter the reflectron. The ion with the higher kinetic energy penetrates deeper into the field and thus has a slightly longer flight path, and in effect reaches the detector more simultaneously with the ions with the lower kinetic energy (Figure 1.4c). Since its introduction, more advanced dual-stage reflectrons have been produced. With a reflectron-TOF in combination with either delayed extraction (in MALDI) or orthogonal acceleration (with continuous ion sources, such as ESI), a mass resolution in excess of 15 000 (FWHM) can be readily achieved, enabling accurate mass determination (<3 ppm) [57]. Currently, commercial TOF-MS systems are available with a mass resolution in excess of 70 000 (FWHM).

#### 1.4.5

##### Fourier Transform Ion Cyclotron Resonance Mass Spectrometer

A Fourier-transform ion cyclotron resonance mass spectrometer (FT-ICR-MS) can be considered an ion-trap system, where the ions are trapped in a magnetic rather than in a quadrupole electric field. The ICR (ion-cyclotron resonance) cell is positioned in a strong magnetic field  $B$  (up to 15 T). The cylindrical or cubic ICR cell consists of two opposite trapping plates, two opposite excitation plates, and two opposite receiver plates (Figure 1.4d). The ions with  $m/z$  describe circles with radius  $r$  perpendicular to the magnetic field lines. This results in a cyclotron frequency  $\omega_c = 2\pi f = v/r = Bez/m$ , where  $f$  is the frequency in Hertz. The cyclotron frequency is thus inversely proportional to the  $m/z$  value. The ions, trapped in their cyclotron motion in the cell, are excited by means of an RF pulse at the excitation plates. As a result, the radius of the cyclotron motion increases and ions with the same  $m/z$  values start moving in phase. The coherent movement of the ions generates an image current at the receiver plates. The image current signal decays in time, because the coherency of the ion movement is disturbed in time. The time-domain signal from the receiver plates contains all frequency information of the ions present in the cell. By Fourier transformation, the time-domain signal is transformed into a frequency-domain signal, which can then be transformed into a mass spectrum [10, 58]. As ion trapping is involved in FT-ICR, concerns with space-charging effect are valid as well.

FT-ICR-MS instruments provide extremely high (mass-dependent) resolution, typically in excess of  $10^5$  (FWHM), accurate mass determination ( $\leq 1$  ppm), and a dynamic range of five orders of magnitude. The resolution increases with measurement time, and longer measurement times are only possible if extreme high vacuum ( $\sim 10^{-9}$  mbar) is achieved in the ICR cell. Higher spectrum acquisition rates can be achieved in instruments with a higher magnetic field strength, that is, the same high-resolution spectrum can be achieved in a shorter time. At present, commercial FT-ICR-MS systems are available that provide a resolution of  $\sim 650\,000$  (at  $m/z$  400, FWHM) at 1 spectra per second. For many years, FT-ICR-MS was primarily used in fundamental studies of gas-phase ion-molecule reactions. However, because of its high-resolution capabilities, FT-ICR-MS in combination with ESI is an ideal tool for the characterization of large biomolecules [59]. At present, FT-ICR-MS plays an important role in top-down strategies to characterize proteins [60, 61] (see Section 1.6.6).

#### 1.4.6

##### Orbitrap Mass Analyzer

Similar to FT-ICR-MS, the acquisition of mass spectra in an orbitrap MS is based on the Fourier transformation of image currents of trapped ions. However, in the orbitrap, no magnetic field is involved. The ions perform an axial oscillation while rotating around a cylindrical inner electrode. The image currents are detected by the two outer electrodes (Figure 1.4e). The mass spectra are generated by Fourier transformation of the time-domain signals into the frequency-domain signals. The  $m/z$  value is inversely proportional to the square of the frequency. Orbitrap instruments, which have been introduced only recently [10, 45, 62], allow ultra-high-resolution measurements (in excess of  $10^5$ , FWHM) at relatively high speed. Although a stand-alone version of the orbitrap has been produced [63], in most cases hybrid systems are applied (see Section 1.5.8).

An important practical aspect to orbitrap MS performance is the adequate delivery of ions into the orbitrap. In commercial systems, this is done in a pulsed way by means of a C-trap, which is essentially a curved high-pressure quadrupole capable of trapping ions and sending them as a concise ion package into the orbitrap [45, 62]. A schematic diagram of the instrumental setup is shown in Figure 1.4e.

Similar to FT-ICR-MS, the mass resolution of an orbitrap improves with longer measurement times. However, significant progress has been made recently in improving the acquisition rates. Whereas initial commercially available orbitrap systems needed  $\sim 1.6$  s to achieve a resolution of 100 000 (at  $m/z$  200, FWHM), more recent systems can achieve a resolution of 140 000 (at  $m/z$  200, FWHM) in 1 s, and an orbitrap-based system enabling a resolution of 450 000 (at  $m/z$  200,

FWHM) has been described as well. This enables accurate mass determination with an accuracy within 1 ppm.

#### 1.4.7

### **Ion Detection**

Different types of ion detection devices are in use. All ion detection systems must be backed by sufficiently fast electronics, including analog-to-digital converters (ADCs), to enable the high-speed data acquisition required in MS [44].

The most widely applied detection system is an electron multiplier, based on the repeated emissions of secondary electrons, resulting from the repeated collisions of energetic particles at a suitable surface. The electron multiplier may be either of the discrete dynode type or of the continuous dynode type [64]. The typical gain of an electron multiplier is  $10^6$ . The electron multiplier is used in combination with quadrupole, ion-trap, and sector instruments. They have limited lifetime ( $\sim 1$ – $2$  years). A conversion dynode, held at a high potential (5–20 kV), is positioned in front of the multiplier, to enable the detection of negative ions and to increase the signal intensity of ions, especially in the high-mass region.

With TOF instruments, microchannel plate (MCP) detectors are applied, as they are more suitable for ion detection when the ion beam is more spread in space. An MCP is an array of miniature electron multipliers oriented parallel to one another, often with a small angle to the surface [65]. In order to generate a spectrum from ion arrival events in TOF instruments, either a time-to-digital converter (TDC) or an ADC is applied. TDCs provide excellent time resolution and low random noise, but do not discriminate in the intensity of the pulse. High ion densities may lead to saturation effects. In an ADC, the integrated circuit chip receives a time-dependent signal and generates a typically 10-bit digital output: both arrival time and the number of colliding ions are recorded. ADCs can provide 1–4 GHz time resolution and discriminate 1024 different ion intensity levels.

In FT-ICR-MS and orbitrap MS systems, ion detection is based on the detection of high-frequency image currents if the ions move coherently, as described in Sections 1.4.5 and 1.4.6 [58]. The signals of all ions, that is, with different  $m/z$  values, are detected simultaneously.

## 1.5

### **Tandem Mass Spectrometry**

#### 1.5.1

#### **Introduction: “Tandem-in-Time” and “Tandem-in-Space”**

In tandem mass spectrometry (MS–MS), two mass analyzers are combined in series (in time or space, see below) with a reaction chamber in between. The  $m/z$  values of ions are measured before and after the reaction within the reaction chamber. In most cases, a change in mass and thus in  $m/z$  is involved, although

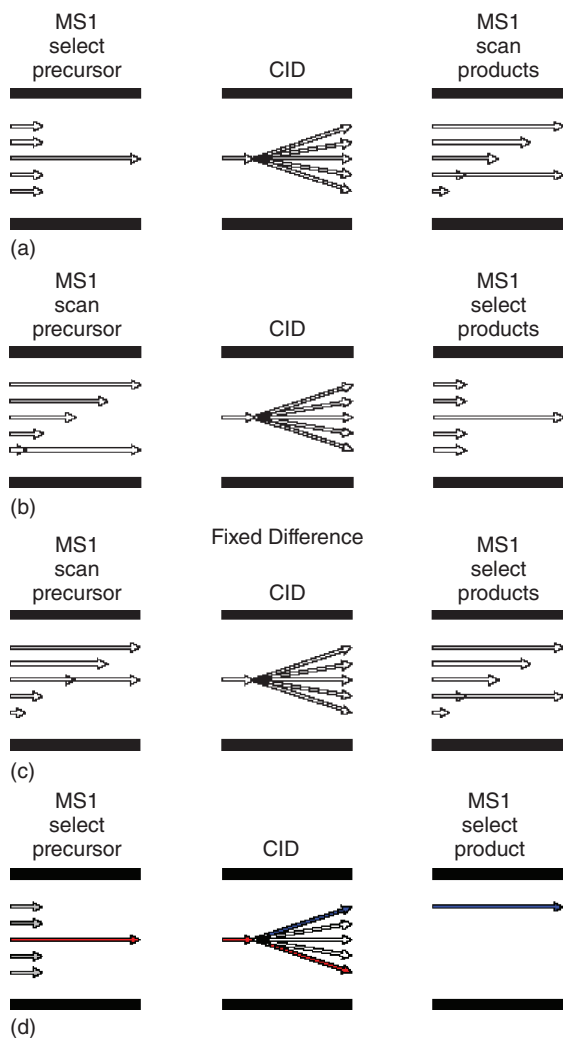


**Figure 1.5** Analysis modes of an MS–MS instrument (“tandem-in-space”), with (a) product-ion analysis, (b) precursor-ion analysis, (c) neutral-loss analysis, and (d) selected-reaction monitoring mode.

a change in charge, for example, charge stripping of multiple-charge ions, is also possible. For positive ions, the precursor or parent ion  $m_p^+$  is converted into the product or daughter ion  $m_d^+$  via the loss of a neutral fragment  $m_n$ . Whereas the neutral fragment  $m_n$  is not detected, its mass can be deduced from the  $m/z$  difference of  $m_p^+$  and  $m_d^+$ . In the product ion analysis mode (see Figure 1.5a), which is the most basic MS–MS experiment, the precursor ion  $m_p^+$  is selected in the first stage of mass analysis (MS1), while the product ions  $m_d^+$  are mass-analyzed and detected in the second stage (MS2) [66].

The historical starting point of MS–MS is the observation and explanation in the 1940s of the occurrence of metastable ions in a magnetic-sector instrument [67]. Subsequently, it was discovered that the abundance of the metastable ions can be increased by energetic collisions in a collision cell. From the mid-1970s onward, instruments were especially designed for MS–MS, for example, triple-quadrupole (TQ) instruments [68], multistage MS–MS in ion-trap instruments [69], hybrid quadrupole–time-of-flight instruments (Q–TOF) [70], hybrid quadrupole-linear ion-trap instruments (Q–LIT) [47], TOF–TOF instruments [71], and hybrid LIT–orbitrap instruments [45, 62].

The MS–MS instrument includes a combination of two mass analyzers. The first and second stage of mass analysis may be performed by the same type of mass analyzer, as in a TQ or an ion-trap instrument. In TQ instruments, the three steps of the MS–MS process, that is, the precursor ion selection, collision-induced dissociation (CID; see Section 1.5.2), and mass analysis of the product ions, are performed in spatially separated devices (“tandem-in-space”), whereas in an ion-trap instrument, the three steps are performed one after another in the same device (“tandem-in-time”) [72]. In a hybrid instrument, the first and second stage of mass analysis are performed in two different types of mass analyzers, for example, a first-stage quadrupole and second-stage linear ion trap in a Q–LIT instrument, or in a first-stage quadrupole and second-stage TOF in a Q–TOF instrument.

An MS–MS instrument allows studying the fragment ions of selected precursor ions and is therefore an indispensable tool in fundamental studies on ion generation, ion–molecule reactions, unimolecular fragmentation reactions, and identity of ions. It plays an important role in qualitative analytical applications of MS involving the on-line coupling of MS to GC (gas chromatography) or LC, for example, in the identification of drug metabolites (Section 1.6.4) or in peptide sequencing (Section 1.6.6) and protein identification (Section 1.6.7).

### 1.5.2

#### **Ion Dissociation Techniques**

MS–MS is based on the gas-phase dissociation or fragmentation of selected ions. It may involve either metastable ions or activated ions. Metastable ions are ions with sufficient internal energy that survive long enough to be extracted from the ion source before they fragment, but may then fragment in the mass analyzer region before detection. The charged fragments of metastable ions may be detected, for example, using various linked-scan procedures in double-focusing sector instruments [44, 66]. However, fragmentation may also be induced by activation of selected ions, that is, by increasing their internal energy. The most widely applied method of ion activation is collisional activation. On acceleration and collision of the selected ions with a target gas (He, N<sub>2</sub>, or Ar) in a collision cell, the ion translational energy can partially be converted into ion internal energy. If subsequent dissociation of the ion occurs in the collision cell, the process is called *collision-induced dissociation*. CID is a two-step process: after converting ion translational energy into ion internal energy in an ultrafast collision event

( $\sim 10^{-15}$  s), unimolecular decomposition of the excited ions may yield various product ions by competing reaction pathways. CID can be performed in two different energy regimes [73]. Low-energy CID is performed in most instruments. During the residence time in the collision cell, the selected precursor ions undergo multiple collisions with a target gas ( $\sim 10^{-3}$  mbar He, N<sub>2</sub>, or Ar). In sector and TOF–TOF instruments, high-energy CID can be performed, involving single kilo electron-volts collisions with He as target gas. High-energy collisions may result in more informative and more complex MS–MS spectra, because a wider range of fragmentation reaction pathways is opened. In the low-energy CID regime, one may further discriminate between collision-cell CID and ion-trap CID. In collision-cell CID, applicable to TQ and Q–TOF instruments, collisions are performed with N<sub>2</sub> or Ar after acceleration of the precursor ions with 10–60 V. In ion-trap CID, collisions are performed with a smaller target (He instead of Ar), ion excitation is achieved by an RF waveform pulse, and the interaction time is milliseconds in ion-trap CID rather than microseconds [50].

Various other ion activation methods have been used, mostly in specific applications and/or instruments [73, 74]. Some of these methods are primarily developed to induce fragmentation in FT-ICR-MS instruments, for example, infrared multiphoton photodissociation (IRMPD), sustained off-resonance irradiation (SORI), and black-body infrared radiative dissociation (BIRD) [73, 74]. Others such as surface-induced dissociation and laser photodissociation have been used on various instruments, but mostly by a limited number of research groups. Currently, the most widely applied alternative ion-activation methods are electron-capture dissociation (ECD) and electron-transfer dissociation (ETD) [75, 76]. A nice comparison of some of these ion dissociation techniques has been reported for glycopeptide analysis [77].

ECD is based on the interaction of multiple-charge protein ions with low-energy free electrons ( $\sim 1$  eV) in an FT-ICR cell, resulting in the formation of multiple-charge odd-electron ions,  $[M+nH]^{(n-1)+\bullet}$  [78]. In CID, peptides predominantly show backbone fragmentation at the peptide bond, resulting in the so-called *b* and *y'* ions [79] (see also Section 1.6.6). In ECD and ETD, cleavage of the N–C<sub>α</sub> bond is observed, thus resulting in even-electron *c'* and odd-electron *z'* ions. Moreover, in ECD, labile bonds to posttranslational modifications such as glycans and phosphates are mostly preserved [75]. The low-energy electrons used in ECD are generally generated from an (indirectly heated) electron-emitting surface. In ETD, the peptide fragmentation is induced by transfer of electrons from radical anions of compounds such as fluoranthene to the multiple-charge ions [76, 80]. ETD is more readily implemented on other type of mass analyzers such as ion-trap, Q-TOF, and orbitrap instruments [75].

### 1.5.3

#### Tandem Quadrupole MS–MS Instruments

Probably the most widely used MS–MS configuration is the TQ instrument, where mass analysis is performed in the first and third quadrupoles, while the

second quadrupole is used as a collision cell in the RF-only mode, that is, in a  $Q-q_{\text{coll}}-Q$  configuration [68]. Although usually called a *triple-quadrupole instrument*, because of the initial lineup of two analyzing quadrupoles and a quadrupole collision cell, the term tandem quadrupole (TQ) would nowadays be more appropriate to describe most of the commercially available instruments. The gas-filled RF-only collision cell, which provides refocusing of ions scattered by collisions, results in significant transmission losses. In attempts to reduce these losses, alternative RF-only collision cells have been developed, for example, RF-only hexapoles or octapoles. In a linear-acceleration high-pressure collision cell (LINAC), an axial voltage and tilted rods are used to reduce the residence time of the ions in the collision cell and to reduce crosstalk [81]. Crosstalk may occur on rapid switching between two selected-reaction monitoring (SRM, see below) transitions with the same product ion from two different precursor ions. Product ions of the first precursor ion are erroneously attributed to the second precursor ion, because these still reside in the collision cell while MS1 is already switched to the second precursor ion. A stacked-ring collision cell, featuring an axial traveling-wave or transient DC voltage to propel the ions and to reduce the transit times, has been reported as well [15].

The introduction and wide application of soft-ionization techniques such as ESI has in fact greatly stimulated the use of MS–MS. The most frequently applied MS–MS data acquisition mode is SRM, applied in routine targeted quantitative analysis [82]. In the SRM mode (see Figure 1.5d), both stages of mass analysis perform the selection of ions with a particular  $m/z$  value. In MS1, a precursor ion is selected, mostly the protonated or deprotonated molecule of the target analyte. The selected ion is subjected to dissociation in the collision cell. In MS2, a preferably structure-specific product ion of the selected precursor is selected and detected. Thus, an SRM transition is a combination of a precursor ion  $m/z$ , a product ion  $m/z$ , and all MS parameters, for example, collision energy, required to measure this transition with the best sensitivity in a particular TQ instrument. Because of the high selectivity involved in SRM, excellent sensitivity may be achieved in target quantitative analysis (see Section 1.6.2). The SRM mode is the method of choice in quantitative bioanalysis using LC–MS, for example, in (pre)clinical studies for drug development within the pharmaceutical industry [83–85], and is also widely used for targeted quantitative analysis in many other application areas, including environmental, food safety, and clinical analysis. It has also been implemented in quantitative analytical strategies using GC–MS as well [86]. The SRM mode is frequently (but erroneously) called “*multiple-reaction monitoring*” (MRM) to indicate that multiple product ions of one precursor ion are monitored, even when only one product ion is monitored. In addition to SRM, various structure-specific screening procedures for the TQ instruments were introduced, for example, the precursor ion analysis (PIA) and neutral-loss analysis (NLA) mode [87, 88] (see Section 1.6.1 and Figure 1.5b,c).

## 1.5.4

**Ion-Trap MS<sup>n</sup> Instruments**

An ion-trap instrument provides three features, which makes it ideally suited for MS–MS. It has the possibility to  $m/z$ -selectively eject ions from the trap, it is operated with a constant He pressure in the trap that may serve as collision gas, and it is possible to apply an  $m/z$ -selective RF waveform to the end-cap electrodes to excite ions of the selected  $m/z$  [50]. In ion-trap MS–MS, one starts with a population of ions, from which the precursor ion is selected, excited, and fragmented, resulting in a new population of (product or daughter) ions. The latter population can be scanned out to be detected, or can serve in a new series of subsequent steps of the process: selection of a product ion as precursor ion in a new MS–MS experiment, which is to be excited and fragmented, leading to a new population of (granddaughter) ions. Excitation means that the selected ions move with wider amplitude, and thus at greater speed, through the ion trap. This leads to more energetic collisions with the He bath gas, which in turn leads to a gain in ion internal energy and subsequent fragmentation of the excited precursor ion. The various steps of the process are performed one after another in the same space (the ion trap), and can thus be considered to be “tandem-in-time” [72]. The process described can be repeated to achieve multiple stages of MS–MS or MS<sup>n</sup> (up to 10 stages in most instruments).

As indicated in Section 1.5.2, the ion-trap CID process differs from collision-cell CID: smaller target, RF ion excitation, and longer interaction time. As a result, different fragmentation pathways may be accessible in ion-trap CID compared to collision-cell CID, especially in fragmenting fragment ions in MS<sup>n</sup> experiments. For some compounds, for example, glycosylated saponins [89], stepwise fragmentation can be achieved, for example, subsequent losses of sugar monomers in subsequent MS–MS steps (Figure 1.6). The lower energy involved in ion-trap CID facilitates the acquisition of a wealth of structural information, for example, by stepwise fragmentation and the generation of fragmentation trees [90]. A fragmentation tree is generated by further fragmenting selected fragment ions of a particular stage of MS<sup>n</sup> into the next stage, that is, MS<sup>n+1</sup>. This provides a wealth of information in structure elucidation and identification of unknowns, as is clearly demonstrated for polyphenols [91].

## 1.5.5

**Tandem TOF (TOF–TOF) Instruments**

MALDI is considered to be a soft-ionization technique. However, considerable fragmentation of MALDI-generated ions occurs after acceleration; that is, metastable ions are generated. This process is sometimes indicated as laser-induced dissociation [92]. Obviously, the fragmentation of metastable ions can be induced by additional (high-energy) collisions in a collision cell, which may also result in CID. In MALDI-TOF-MS terms, the process of fragmentation of metastable ions is frequently called post-source decay (PSD) [93]. The kinetic

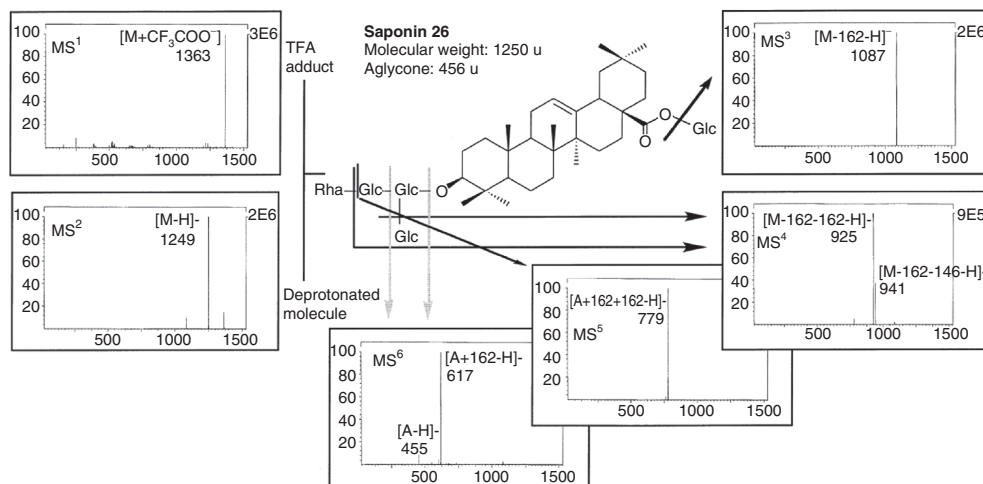


**Figure 1.6** LC-MS<sup>n</sup> in an ion-trap instrument: stepwise fragmentation of glucosylated Saponin 26. (Reprinted with permission from Ref. [89]. ©1998, Elsevier Science.)

energy of these fragment ions  $m_d$  in PSD significantly differs from that of the parent ions  $m_p$ , whereas their velocities are the same. The difference in kinetic energy is proportional to  $m_d/m_p$ . They also suffer from a wide ion kinetic energy distribution. Therefore, these fragment ions are not observed in the TOF-MS process, unless specific actions are taken, including the use of a gridless curved-field reflectron or a reflectron with a time-dependent field. A linear-TOF experiment can be used to measure the precursor ions, whereas a number of reflectron-TOF experiments are needed to acquire the wide-range product ion spectrum. Finally, the product ion mass spectra have to be concatenated by the data system [93].

The problems with the different kinetic energies of precursor and products ions, described above, can also be solved by decelerating the precursor ions before dissociation, for example, from 20 keV down to 1–2 keV, and then re-accelerating the product ions generated in a collision cell. This is generally done, in one way or another, in a TOF-TOF system [94]. MALDI-TOF-TOF-MS systems can currently be routinely applied to acquire MS-MS information from MALDI-generated ions, for example, in proteomics and glycomics [30, 95, 96].

### 1.5.6

#### Hybrid Instruments (Q-TOF, Q-LIT, IT-TOF)

In this section, three types of hybrid MS-MS systems are discussed, two with TOF mass analyzers as MS2 and one with a LIT in MS2.

The Q-TOF instrument can be considered as a modified TQ instrument, where the MS2 quadrupole has been replaced by an orthogonal-acceleration reflectron-TOF mass analyzer [70]. That means that in MS mode, the quadrupole (MS1) is operated in RF-only mode and the RF-only collision cell with low

collision energy, whereas in MS–MS mode the quadrupole performs the selection of the precursor ion with unit-mass resolution and fragmentation of the precursor ion is achieved in the collision cell. In both modes, the ions are orthogonally accelerated into the flight tube and high-resolution mass analysis is performed in a reflectron-TOF analyzer (MS2). Q–TOF instruments are now available from various instrument manufacturers [57]. They are widely used in structure elucidation and biomacromolecule sequencing (see Section 1.6). Because collision-cell CID is applied, the fragmentation characteristics are the same as in TQs. In structure elucidation, a significant advantage of Q–TOF is the ability to perform accurate mass determination (<5 ppm) for both precursor and product ions. Principles and applications of Q–TOF hybrid instruments have been reviewed [97, 98].

Hybrid MS–MS instruments have been developed, featuring ion traps in either the first (MS1) or the second stage of mass analysis (MS2). If the ion trap is implemented as MS1, it generally acts as a “filter” with respect to the number of ions that is transferred to MS2, based on the duration of the ion accumulation in the ion trap. In addition, MS<sup>n</sup> experiments may be performed before transferring a package of ions to MS2. Thus, in such hybrid systems, no collision cell has to be present between the first and second stage of mass analysis. This is true for ion-trap hybrids with FT-ICR-MS (see Section 1.5.7) and orbitrap (see Section 1.5.8) instruments, but also for the hybrid ion-trap-time-of-flight (IT–TOF) system. IT–TOF systems have been pioneered by the group of Lubman [99, 100]. It has subsequently become commercially available for both MALDI and LC–MS applications [101]. It readily provides high-resolution MS and MS<sup>n</sup> data, and has been applied for structure elucidation, for instance, in metabolite identification [101] or otherwise [102]. Unlike CID in other IT devices, where He is used to stabilize the ion trajectories and as collision gas, pulses of Ar are used to prevent precursor ions from being lost from the trap and to perform MS<sup>n</sup> in an IT–TOF instrument.

In the Q–LIT hybrid instruments [47, 103], a (linear) IT is implemented as the second stage of mass analysis (MS2), for accumulation of ions to achieve improved sensitivity after collision-cell CID, and/or to perform MS<sup>3</sup>. The Q–LIT instrument can be operated either as a conventional TQ instrument, where it is capable of all TQ acquisition modes including SRM, or as the hybrid instrument. In the hybrid mode, full-spectrum data can be acquired in the enhanced product ion (EPI) analysis mode with up to 60-fold enhanced sensitivity compared to TQ instruments, while still acquiring collision-cell CID spectra. The system also allows the acquisition of MS<sup>3</sup> spectra, with the second dissociation step to be performed in the LIT [103, 104]. Hardware, electronics, and software control of the Q–LIT instrument have been optimized to allow very rapid switching between various MS and MS–MS experiments. Q–LIT instruments have found wide application in LC–MS.

## 1.5.7

## MS-MS and MSn in FT-ICR-MS

As targeted ions can be selectively trapped in the ICR cell, while unwanted ions can be eliminated by the application of RF pulses, the MS<sup>n</sup> procedures in an FT-ICR-MS instrument greatly resemble those in an ion-trap instrument. However, successful operation of an FT-ICR-MS instrument requires extreme low pressures in the cell ( $\sim 10^{-9}$  mbar). Thus, the vacuum constraints hamper the possibilities of performing CID in the FT-ICR cell [58]. This problem can be elegantly solved either by the use of hybrid systems where fragmentation is performed before transfer of ions to the ICR cell or by the use of alternative ion dissociation techniques. With respect to hybrid systems, both quadrupole-FT-ICR-MS systems [105] and LIT-FT-ICR-MS systems [106, 107] have been described and widely applied. These hybrid systems provide great versatility, user-friendliness, and excellent performance characteristics. With respect to alternative ion-activation methods, IRMPD, SORI, and, more recently, ECD and ETD have been frequently applied (cf. Section 1.5.2).

The potential of FT-ICR-MS in studying biomolecular interactions can be illustrated by some early examples [108, 109]. ESI-MS was used to generate gas-phase ions of noncovalent complexes of 16 benzenesulfonamide inhibitors

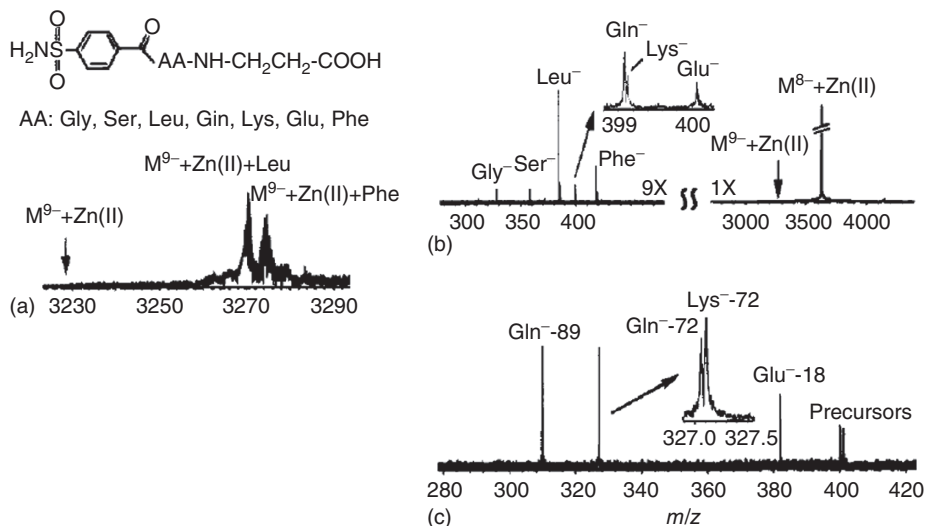


**Figure 1.7** Negative-ion ESI spectra (using FT-ICR-MS) of  $7.0 \mu\text{M}$  bovine carbonic anhydrase II with benzenesulfonamide inhibitors ( $7.0 \mu\text{M}$  each) in  $10 \text{ mM NH}_4\text{OAc}$  (pH 7.0). With (a) the mass spectrum of the  $[9-]$  ion prior to ion isolation, (b) isolation and subsequent CID of the  $[9-]$  ion, where the intensity of dissociated inhibitors correlate with

their binding affinity, and (c) SWIFT isolation of three of the inhibitor ions (from B), Glu-, Lys-, and Gln- at  $m/z$  399–401 and subsequent CID to obtain fragment ions for the inhibitors. (Reprinted with permission from Ref. [108]. ©1995, American Chemical Society.)

with bovine carbonic anhydrase II (BCA-II), which are introduced into the FT-ICR cell (see Figure 1.7). The tightly folded complexes generally formed only two charge states. Complexes of BCA-II were observed with all 16 benzenesulfonamides with relative abundances consistent with the binding constants of the inhibitors in solution. Competition experiments could be performed as well by adding an excess of a high-affinity inhibitor to the electrosprayed solution. For some inhibitors of closely related masses, gas-phase dissociation of the (isolated) complexes was achieved to release the inhibitors, measure their accurate mass, and subsequently perform a second dissociation step to study the fragmentation of the inhibitors (see Figure 1.7) [108]. This approach was coined “bioaffinity characterization mass spectrometry” [109]. It basically comprises three steps: (i) selective accumulation of a noncovalent protein–ligand complex, (ii) gas-phase dissociation of the complex to release the ligand, and (iii) fragmentation of the ligand for further structure elucidation [109].

### 1.5.8

#### Orbitrap-Based Hybrid Systems

Although stand-alone orbitrap systems have been produced, the full power of the orbitrap mass analyzer is achieved by its use in an MS–MS setting. The initial instrumental setup of the orbitrap consisted of a hybrid LIT–orbitrap configuration, featuring an LIT to control the number of ions transferred to the orbitrap and to perform  $MS^n$ , a C-trap to direct the package ions into the orbitrap, and the orbitrap itself (see Figure 1.4e) [45]. As the ion-trap system in this commercial LIT–orbitrap instrument is equipped with separate off-axis detectors, simultaneous acquisition of high-resolution precursor ion and unit-mass-resolution product ion mass spectra can be achieved. If both precursor ions and product ions are detected using the orbitrap, high resolution ( $\sim 100\,000$ , FWHM) is used for the precursor ions, whereas medium resolution ( $\sim 15\,000$ – $30\,000$ , FWHM) is generally sufficient for the product ions of a well-characterized precursor ion.

Later on, it was demonstrated that CID could be achieved in the C-trap, which is a gas-filled quadrupole type of device [110]. The C-trap fragmentation resembles the collision-cell CID more than it resembles the ion-trap–CID. Subsequently, separate higher-energy RF-only collision octapoles (higher-energy collision-induced dissociation, HCD) were mounted on LIT–orbitrap hybrid systems to make optimum use of this feature. Such a system can be considered a gas-phase ion-chemistry laboratory on its own, featuring different ways to perform fragmentation, that is, ion-trap CID, HCD, and eventually ETD, as well as different ways to measure the  $m/z$  values of the resulting ions, that is, by unit-mass resolution with the ion trap or by ultra-high resolution with the orbitrap. In fact, HCD also led to the stand-alone orbitrap [63], mentioned earlier, thus providing the possibility to efficiently fragment ions without precursor ion selection, as well as to hybrid quadrupole–orbitrap systems [111].

Most recently, a tribrid orbitrap-based system was introduced, featuring parallel quadrupole and LIT systems, next to an orbitrap mass analyzer [112].

In this system, precursor ion selection is performed either in the quadrupole or in the LIT. In the former case, fragmentation can take place either in the HCD cell, followed by orbitrap mass analysis, or in the ion trap, followed by mass analysis and detection in either the ion trap or the orbitrap. In the latter case, (eventually multistage) fragmentation takes place in the ion trap, again with mass analysis and detection in either the ion trap or the orbitrap. Fragmentation by HCD is performed in the HCD cell, while ion-trap–CID or ETD can be performed in the ion trap. The high-field orbitrap analyzer implemented provides at a resolution of  $\sim 500$  per ms acquisition time, thus  $\sim 120\,000$  in  $0.26$  s (at  $m/z$  200, FWHM), with a maximum of  $\sim 500\,000$  in  $\sim 1.1$  s (at  $m/z$  200, FWHM).

### 1.5.9

#### Ion-Mobility Spectrometry–Mass Spectrometry

Ion-mobility spectrometry (IMS) is a powerful tool in the study of gas-phase ions [113, 114]. An ion-mobility spectrometer consists of (i) an ion-generation region, mostly a radioactive  $^{63}\text{Ni}$  foil, (ii) a charge-separation region, (iii) an ion shutter, (iv) the actual drift-reaction region, and (v) an ion detector, for example, a mass spectrometer. The ion shutter provides pulse-wise introduction of ions into the drift tube, in which a uniform axial electric field gradient (typically  $1\text{--}1000\text{ V cm}^{-1}$ ) is maintained with a series of guard rings, separated by electrically insulating spacers and connected with an appropriate precision resistor network. The IMS measures how fast a given ion moves through the buffer gas (He,  $\text{N}_2$ , or Ar) in a uniform electric field, and can thus be used to determine (reduced) ion mobility from the drift time. IMS may be considered being gas-phase electrophoresis. Larger ions undergo more collisions with the buffer gas and thus will have longer drift times than smaller ions. Higher charge states of an ion experience a greater effective drift force, and thus show higher mobility than the lower charge states. From the measured reduced mobility, the experimental collision cross section can be determined, after appropriate calibration with reference compounds [115]. Theoretical prediction of the collision cross section, for example, for peptides, is also possible, generally showing good correlation to experimental values [116, 117].

The on-line combination of IMS with MS results in a very attractive tool to combine analysis of conformation and shape, as performed in IMS, with the analysis of  $m/z$  and structural features, as performed in MS. IMS–MS has been pioneered by the groups of Bowers [118] and Clemmer [119, 120], developing IMS interfaced to quadrupole or TOF instruments. IMS–MS provides a rapid gas-phase separation step before MS analysis, enabling the identification of ions with different drift times, thus with different collisional cross sections. Instrumental developments in IMS–MS have been reviewed [121]. IMS–MS is extensively used to study gas-phase protein conformations, for instance, in relation to neurodegenerative and neuropathic diseases such as Parkinson's and Alzheimer's disease [122]. Currently, there are three ways to implement IMS in IMS–MS.

The groups of Bowers and Clemmer [118, 119, 123] use the type of drift tubes also applied in stand-alone IMS. Whereas the conventional drift-tube approach has been the first way to perform ion mobility in combination with MS, drift-tube IMS–MS systems have become commercially available only very recently (2014). Nevertheless, successful application of this type of IMS–MS instruments has been demonstrated from various other laboratories as well for both small molecules and biomacromolecules [121–124].

A successful alternative approach to IMS–MS is based on the use of traveling-wave stacked-ring ion guides, which were initially developed to replace RF-only hexapole ion guides in vacuum interfaces for API or as collision cells [15, 125]. To this end, a Q–TOF instrument featuring traveling-wave ion guides in both the vacuum-interface region and the collision-cell region was constructed. Initially, ion-mobility spectra were acquired by storing ions in the ion-source ion guide and gating them periodically to the collision-cell ion guide, operated at a 0.2-mbar pressure of Ar. The mobility-separated ions were subsequently analyzed using the TOF-MS system [15]. The initial setup was developed into a hybrid Q–IMS–TOF instrument [125]. The collision-cell region of this instrument features three traveling-wave stacked-ring ion guides, of which the middle one is used as a 185-mm-long ion-mobility drift tube, operated at pressures up to 1 mbar and up to 200 ml Ar gas, and the other two may be used as 100-mm-long collision cell, operated at  $10^{-2}$  mbar when applicable. The system can be applied for a wide variety of ion-mobility studies, such as protein conformation studies [122] and differentiation of heterogeneities in glycoproteins [126].

A third way to perform IMS–MS is high-field asymmetric waveform ion-mobility spectrometry (FAIMS) [127–129]. In FAIMS, the gas-phase mobility separation of ions in an electric field is achieved at atmospheric pressure. In its simplest design, the FAIMS device comprises two parallel rectangular electrodes at a uniform distance. One of the electrodes is grounded, while at the other an asymmetrical waveform is applied, characterized by a significant difference in voltage in the positive and negative polarities of the waveform. Ions drift through the gas between the electrodes and are separated depending on their mobility. Whereas at low field the ion mobility is proportional to the field strength, at high field the ion mobility becomes dependent on the applied electric field. Because of the applied asymmetric waveform, the ions show a net displacement toward the grounded plate, which, however, is compensated for by a DC voltage (compensation voltage). This ensures that the ions remain between the plates. Scanning of the compensation voltage allows ions with different mobilities to be monitored. Next to the ion-mobility separation of the ions, focusing of the beam is achieved, thus improving the sensitivity in an FAIMS–MS system. Currently, a variety of (often cylindrical) electrode configurations are applied [127–129]. Commercially available FAIMS devices are primarily applied to improve sensitivity and to reduce matrix effects in quantitative analysis using LC–ESI-MS [129, 130].

In its various forms, IMS–MS plays an important role in many forefront application areas of biological MS, including structural proteomics [131, 132],

characterization of protein assemblies [133], and chiral and structural analysis of biomolecules [134].

## 1.6

### Data Interpretation and Analytical Strategies

#### 1.6.1

##### Data Acquisition in MS Revisited

As indicated in Section 1.2.4, the two basic acquisition modes of MS are the full-spectrum mode and the selected-ion mode. The full-spectrum acquisition mode is applicable to all mass analyzers, in MS, MS–MS, and MS<sup>n</sup> modes. The full-spectrum mode in MS–MS and MS<sup>n</sup> is the product ion analysis mode (Section 1.5.1). The selected-ion acquisition mode, that is, SIM in single-MS instruments and SRM in MS–MS instruments, is a powerful tool in especially the beam instruments, that is, quadrupole and sector instruments, to improve S/N in targeted analysis by elongating the dwell time at a particular  $m/z$ . The resulting data are somewhat comparable to XICs (Figure 1.1c), but often with better S/N than when acquired in full-spectrum mode. Although ion-trapping devices, both ion-traps and FT-ICR-MS systems, can perform a selected-ion acquisition mode as well, the gain in S/N will generally be less than in beam instruments under similar conditions. In TQ instruments, SRM is a powerful tool to greatly enhance selectivity, and thereby achieve excellent lower limits of quantification in targeted quantitative analysis (see Section 1.6.2). In HRMS, especially demonstrated for TOF and orbitrap instruments, post-acquisition narrow-window XIC is a powerful tool to achieve excellent S/N in targeted quantitative analysis. Recently, a high-resolution variant of SRM was proposed, involving the post-acquisition use of accurate mass product ions in MS<sup>2</sup> (see Section 1.6.2).

Another powerful data acquisition mode is the DDA mode (also called *information-dependent acquisition*) [135, 136]. In DDA, the instrument performs a rule-based automatic switching between a survey and a dependent mode. The most widely applied DDA experiments switches between full-spectrum MS survey mode and a full-spectrum product ion (MS–MS) analysis dependent mode, but switching between SRM as a survey mode and product ion analysis as a dependent mode, for instance, is also demonstrated (see Section 1.6.4 for an example). The switching is controlled by the intensity of a possible precursor ion observed and eventually by additional criteria such as isotope pattern, charge state, specific  $m/z$  values on an inclusion list or an exclusion list. In this way, highly efficient data acquisition is possible: MS and MS–MS data of unknown compounds in a mixture are acquired simultaneously in one chromatographic run. An alternative to DDA is data-independent acquisition (MS<sup>E</sup>) [137], where scanwise switching between MS and MS–MS is performed to obtain fragments for all precursor ions present. The MS<sup>M</sup> approach, described for LIT–orbitrap instruments, is a bit similar [138]. Both data-dependent and data-independent

acquisition procedures are frequently used in qualitative analysis of mixtures with unknown constituents, for instance, in metabolite identification (see Section 1.6.4) and proteomics (see Section 1.6.7) workflows.

In “tandem-in-space” instruments, two other data acquisition modes can be performed, that is, the PIA and the NLA modes (see Figure 1.5b,c), which are especially powerful for the screening for related structures in complex mixtures. It allows screening for compounds that on CID show either a characteristic fragment ion (in PIA mode) or a characteristic neutral loss (in NLA mode). In the PIA mode, MS1 is continuously scanned, while in MS2 a characteristic fragment ion is selected and detected. In PIA mode, a signal is detected if an ion transmitted in MS1 on CID generates the common product ion selected in MS2. In the PIA mass spectrum, peaks are shown with their precursor ion  $m/z$  value. An early example of PIA involves the screening for phthalate plasticizers in environmental samples by means of the common fragment ion with  $m/z$  149, due to protonated phthalic anhydride [87]. In the NLA mode, both MS1 and MS2 are scanned, but with a fixed  $m/z$  difference. In NLA mode, a signal is detected if an ion transmitted in MS1 on CID loses a neutral molecule with a mass fitting the fixed  $m/z$  difference. An early example of NLA is the monitoring of  $\text{CO}_2$  losses from deprotonated aromatic carboxylic acids [87]. NLA and PIA are frequently applied in drug metabolism studies (see Section 1.6.4) [139] and in phosphoproteomics [140].

## 1.6.2

### Quantitative Bioanalysis and Residue Analysis

LC–MS on a TQ instrument operated in SRM mode is the gold standard in routine quantitative analysis, as, for instance, performed in pharmacokinetics/pharmacodynamics (PKPD) and absorption, distribution, metabolism, excretion (ADME) studies during drug discovery and drug development by the pharmaceutical industry and related contract-research organizations [83–85]. Whereas in such pharmaceutical applications just one SRM transition per compound is applied, in many areas of quantitative analysis at least two SRM transitions per compound are applied. The latter can be attributed to protocols issued by regulatory bodies, defining procedures in residues analysis [141, 142], which demand not only quantitative analysis of a target compound, but also confirmation of its identity, based on retention time, precursor and product ion, and intensity ratio between two specific ions, for example, two compound-specific SRM transitions. This protocol, initially made for the analysis of veterinary drug residues in food of animal origin, has been widely adapted in other areas of residue analysis, for example, for pesticide analysis in fruits and vegetables and in drinking water, in sports doping, and in forensic/toxicological analysis. Strengths and weaknesses of such an approach have been critically assessed [143, 144]. Perhaps the most obvious limitation of this approach in residue analysis is that a targeted method is applied to search for “in principle” unknown contaminants.

More recently, the use of HRMS has been advocated as an alternative to the targeted approach based on SRM transitions and TQ instruments [57, 145]. The

approach is sometimes called a *qual/quant strategy*. HRMS provides the possibility to acquire full-spectrum data at up to 50 spectra per second and yields accurate mass data. The analysis is untargeted and does not need prior optimization of (multiple) SRM transitions. It also provides the possibility for post-acquisition data mining and retrospective analysis, for example, to search in already acquired data for the presence of a later discovered metabolite or previously not anticipated contaminant. Initial limitations of HRMS in quantitative analysis in terms of lower limit of quantitation and linear dynamic range have been greatly removed by recent technological developments.

### 1.6.3

#### Identification of Small-Molecule “Known Unknowns”

Identification of unknowns may be directed to either “known unknowns” or “unknown unknowns.” The term *known unknown* was introduced to indicate compounds that are unknown to the researcher, but actually described somewhere in the scientific literature and/or available in compound databases [146]. The “known unknowns” differ from the target compounds searched for in targeted residue analysis, described in Section 1.6.2, which can be considered as “known knows.” The identification of “known unknowns” is a highly challenging task, even more so for “unknown unknowns.” This task can generally not be performed by using MS technologies alone, especially because MS often is not a very powerful tool in clearing stereoisomerism issues. Thus, in this, MS analysis should be combined with other techniques, especially nuclear magnetic resonance (NMR) spectroscopy. In practice, this is not straightforward, if one keeps in mind that NMR needs ~100–1000 times more (pure) compound to get an interpretable spectrum. Besides, MS and MS<sup>n</sup> are readily performed within the timescale of high-resolution chromatography, whereas NMR requires far longer data acquisition times, typically 8–16 h when only low concentrations are available. Thus, either fraction collection or time-consuming stop-flow operations have to be performed, when multiple unknowns within one LC run are to be identified by NMR.

The general procedure of the identification of unknowns consists of a number of steps, which primarily are described for “known unknowns” [7, 146, 147]. (i) One needs to collect as much information on the unknowns as possible. Parameters such as origin of the sample, solubility, thermal stability, and possibly underlying chemistry may provide valuable pieces of information. (ii) One needs to establish whether the sample is actually amenable to MS analysis, by GC–MS in EI mode, LC–MS in either positive-ion or negative-ion mode (or preferably both), MALDI-TOF-MS, or by any of the other available MS techniques. (iii) If the first MS data are acquired by HRMS, the calculation of the elemental composition of the unknown is possible, especially when a soft-ionization technique is applied. (iv) On the basis of the elemental composition and the general information on the unknown, compound databases may be searched for known structures, which will be successful for the “known unknowns,” but not for the “unknown unknowns.”

(v) Subsequently acquired MS–MS or MS<sup>n</sup> data allow filtering the known structures from the database search by checking the observed fragmentation behavior against predicted fragmentation of the database-retrieved structures. In favorable cases, this leads to a (number of) potential structure proposal(s) for the unknown. (vi) In the end, standards should be purchased or synthesized and analyzed to check retention time, fragmentation behavior, and possibly other properties. (vii) For the “unknown unknowns”, the database search did not provide results, thus requiring more complicated de novo data interpretation, possibly incorporating substructure searches. Additional tools such NMR, IR, and others will certainly be necessary to solve the puzzle.

At this stage, as a result it may be reported that a structure proposal for the unknown is available, for which the calculated elemental composition is in agreement with the measured accurate mass of the precursor ion, the main fragments in the product ion spectra could be assigned and seem to agree with the proposed structure, and chromatographic and MS characteristics seem to be in agreement with that of a synthetic standard (or an “known unknowns”). Further experiments may need to be performed, for example, preparative LC in order to collect sufficient material for NMR analysis, to further confirm the structure and rule out isomerism issues.

#### 1.6.4

##### Identification of Drug Metabolites

The structure elucidation of related substances, be it synthesis by-products or degradation products of active pharmaceutical ingredients drug metabolites, or natural products within a particular compound class, can be performed by more or less similar strategies [148–151]. Suitable sample pretreatment and LC methods must be developed for the isolation and separation of the related substances. The acquisition of MS, MS–MS, and/or MS<sup>n</sup> spectra of the parent drug and the thorough interpretation of these spectra is of utmost importance to the success of the study. After the analysis of relevant samples in LC–MS mode and data processing to search for potential related substances, MS–MS or MS<sup>n</sup> have to be acquired. Nowadays, this is mostly done by DDA or data-independent MS<sup>E</sup> procedures, using automatic switching between survey MS and (dependent) MS–MS or MS<sup>n</sup> experiments, preferably using HRMS [57, 150]. Finally, interpretation of the data has to be performed, often followed by additional LC–MS<sup>n</sup> experiments, isolation of particular compounds, synthesis of standards, and NMR analysis.

Drug metabolism is directed at increasing the polarity of the drug to enhance its excretion via the kidneys into the urine. It generally occurs in two steps, that is, first by, among others, oxygenation and dealkylation (Phase I metabolism) and second by conjugation with, for instance, sulfate, glucuronic acid, or glutathione (Phase II metabolism). From an MS point of view, the biotransformation of drugs results in metabolic *m/z* shifts, for example, of –14.052 Da due to demethylation and +15.995 Da due to hydroxylation, or *N*-oxide or sulfoxide formation. From *m/z* shifts in the metabolites, relative to the parent drug, one can often conclude

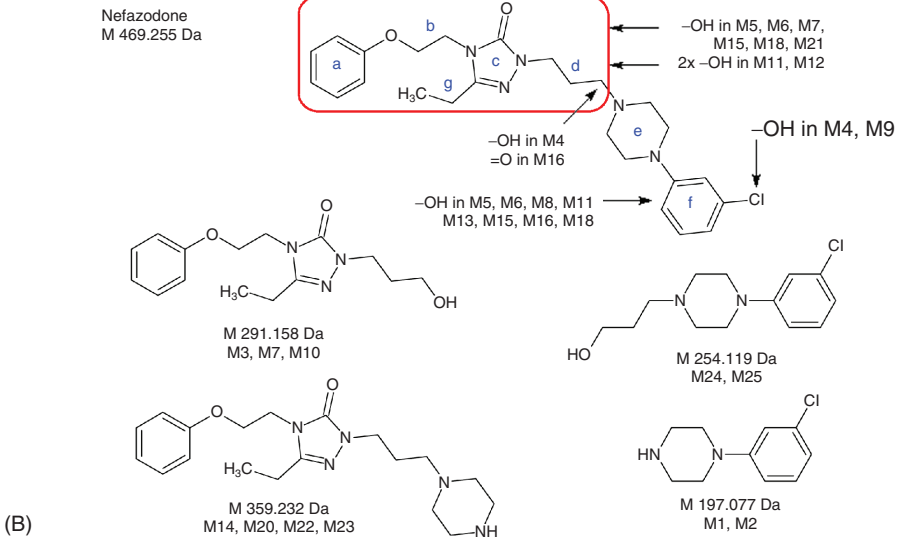
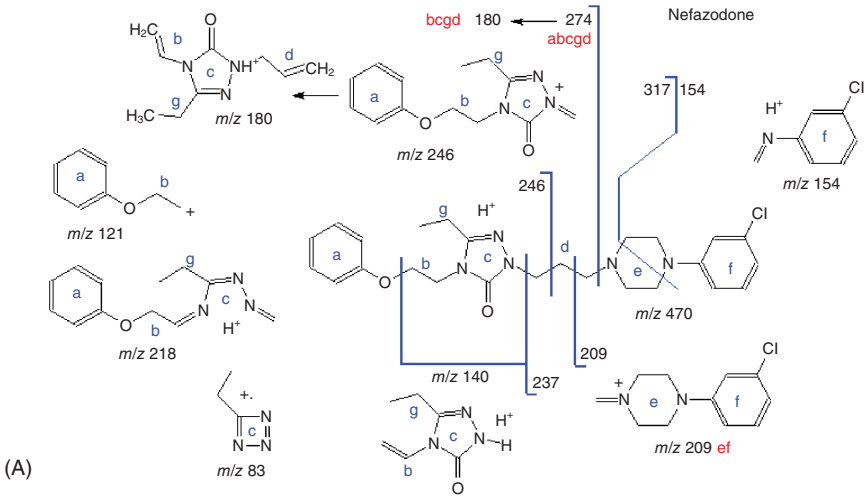
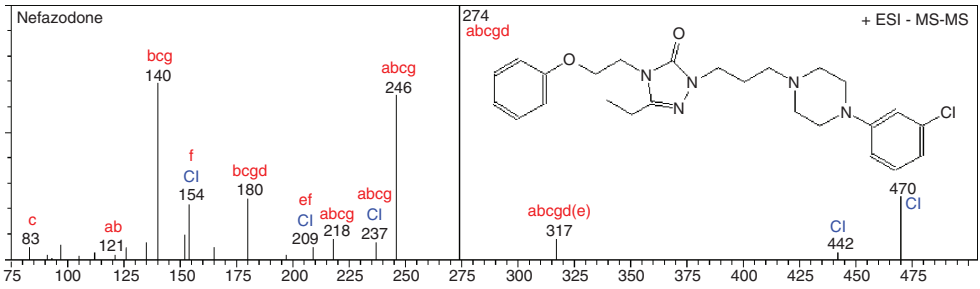
which metabolic change occurred. Understanding of the MS–MS fragmentation of the parent drug allows to keep track of these metabolic shifts in the structure of the compound. To this end, the parent drug can be subdivided into a number of so-called profile groups, to keep track of metabolic  $m/z$  shifts of the precursor ions and to pinpoint them to particular structural elements [152, 153].

The experimental and data interpretation procedures in the identification of *in vitro* drug metabolites may be illustrated for the antidepressant drug nefazodone, which in the past few years has frequently been used to demonstrate advances in LC–MS and MS technology [154–156]. The structure of nefazodone, its MS–MS spectrum, the identity of a number of its fragments, and relevant profile groups are given in Figure 1.8a. Initially, a Q-LIT system was applied to profile and identify as many as 22 nefazodone metabolites, 7 of which were not previously reported [154]. DDA was applied to acquire EPI spectra (see Section 1.5.6). An iterative data processing strategy was applied, based on (i) the recognition of characteristic product ions, for example, the ions with  $m/z$  274 and 140; (ii) the generation of XICs of samples and controls to find possible metabolites; and (iii) the inspection of the product ion spectra of the newly identified metabolites in order both (a) to recognize other characteristic ions that may be used in the generation of additional XICs, for example, the ions with  $m/z$  290, being the oxidized form of the ion with  $m/z$  274, and (b) to identify the metabolites, based on the profile group approach [154]. Subsequently, the identification of the metabolites was confirmed by accurate mass determination using an LIT–orbitrap system. Additional metabolites resulting from N-dealkylation or hydrolysis reactions of large groups were detected as well [155]. An overview of the metabolites found is given in Figure 1.8b. Fourteen out of the 26 identified metabolites involved oxidation (hydroxylation or N-oxidation) of the parent drug. In many cases, the exact position could not be established. It must be pointed out that the described post-acquisition iterative data processing strategy closely resembles an experimental data acquisition strategy based on PIA and/or NLA. Screening for nefazodone metabolites in PIA using the product ions with  $m/z$  246, 274, and 290 (cf., Figure 1.8a) and NLA using constant neutral losses of 196, 224, and 212 Da has also been demonstrated [156]. Another powerful tool in the screening and profiling of drug metabolites is the use of mass-defect filtering (MDF) in HRMS [157]. The metabolic  $m/z$  shifts are accompanied by a shift in the mass defect of the metabolite, for example, of  $-0.0157$  Da due to demethylation and  $-0.0051$  Da due to hydroxylation. If the biotransformation does not lead to major structural changes in the parent drug, for example, N- or O-dealkylation or hydrolysis of large side groups, the mass-defect shifts are limited to  $\pm 40$  mDa for Phase I metabolites and  $\pm 70$  mDa for Phase II metabolites. Software tools have been developed to process HRMS data and to perform MDF within a

---

**Figure 1.8** Metabolite identification of nefazodone. With (A) MS–MS spectrum, interpretation and profile groups of the parent compound nefazodone. (B) Overview of

Phase-I metabolites of nefazodone. MS–MS spectrum of nefazodone redrawn from Ref. [155]. (Reprinted with permission from Ref. [155], ©2007, John Wiley & Sons Ltd.)



$\pm 70$  mDa wide window around the exact  $m/z$  of the parent drug [157]. This has been successfully demonstrated for nefazodone [156]. However, as in the biotransformation of nefazodone, major structural changes do occur (see above), and additional mass-defect filters must be defined and used [156].

In many cases, multiple oxygenated metabolites may be observed. H/D-exchange experiments may be performed to discriminate between C-hydroxylation and N- or S-oxidation. All three types of metabolites show a +15.9949 Da mass shift. The hydroxylated metabolites show H/D exchange, whereas the N- or S-oxidated products do not [158]. Differentiation between various isomeric C-hydroxylated metabolites is often difficult. In this respect, IMS-MS may be of help. For isomeric hydroxylated metabolites, the differences in drift time are generally too small, compared to the resolution of the IMS separation [159]. A selective derivatization of aromatic hydroxyl groups of drug metabolites into *N*-methyl pyridinium derivatives has been demonstrated to sufficiently increase the differences in collision cross sections, and thus in drift times, to allow differentiation between isomeric forms [160]. In an earlier study, the same group differentiated between isomeric glucuronic acid conjugates using IMS-MS [161]. By correlating theoretically predicted collision cross sections to measured drift times of a parent drug and its fragments, a calibration plot was generated, which could subsequently be used to differentiate between chromatographically separated isomeric glucuronic acid conjugates or *N*-methyl pyridinium derivatives.

In total, the described data acquisition and processing strategies form an elaborate toolbox that may be used in profiling and identification of drug metabolites (see Figure 1.9). The acquired full-scan high-resolution MS data sets may be interrogated using XIC, MDF, isotope-pattern filtering (if specific isotopic features, e.g., Cl or Br atoms, are present in the parent drug), and background subtraction, whereas data-dependent and/or data-independent MS-MS and/or  $MS^n$  data sets may be interrogated using product ion filtering or PIA and neutral-loss filtering or NLA [157]. NLA is especially powerful in the screening for Phase II drug metabolites, using constant neutral losses of 80 and 176 Da for sulfate and glucuronic acid conjugates, respectively [139]. The potential of IMS-MS in this area has just started to be explored.

Similar strategies are applied in the screening for reactive metabolites by glutathione trapping [162]. In positive-ion mode, either NLA using losses of 129 Da (pyroglutamic acid) or 307 Da (glutathione) or PIA with the characteristic product ion with  $m/z$  130 (protonated pyroglutamic acid) can be applied to screen for glutathione conjugates, whereas in negative-ion mode PIA using the common fragment ion with  $m/z$  272 can be used [163]. Enhanced selectivity in NLA is achieved in  $MS^E$  with a post-acquisition selection of the precursor ions that show the loss of 129.043 Da, the accurate mass of pyroglutamic acid [164]. Alternatively, SRM-triggered DDA on a Q-LIT instrument can be applied using a wide range of predicted SRM transitions for possible glutathione conjugates [165]. NLA in combination with reactive-metabolite trapping by stable-isotope-labeled or chemically modified glutathione has been another screening strategy [166, 167].

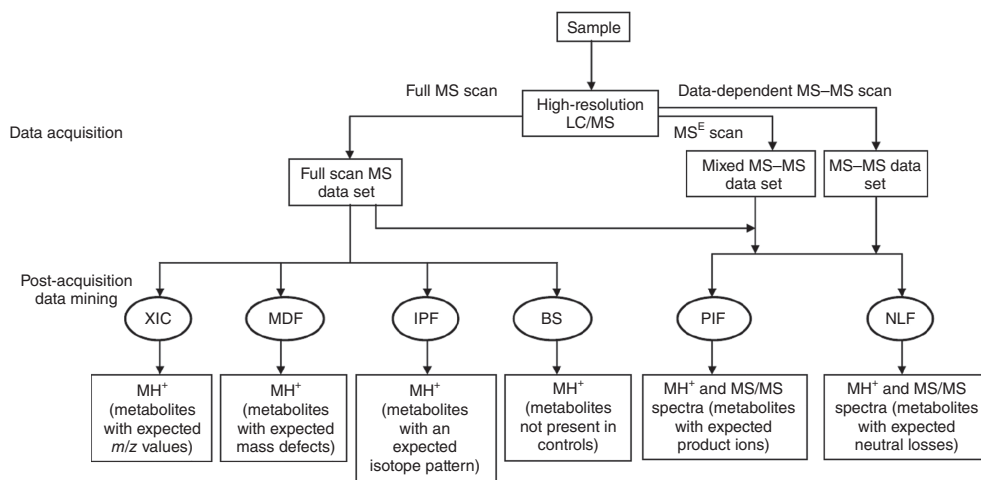


**Figure 1.9** Toolbox for profiling and identification of drug metabolites. The acquired full-scan high-resolution MS data sets may be interrogated using extracted-ion chromatograms (XIC), mass-defect filtering (MDF), isotope-pattern filtering (IPF), and background subtraction (BS), whereas

data-dependent and/or data-independent MS–MS and/or  $MS^n$  data sets may be interrogated using product-ion filtering (PIF) or precursor-ion analysis (PIA) and neutral-loss filtering (NLF). (Reprinted with permission from Ref. [157], ©2009, John Wiley & Sons Ltd.)

Obviously, MDF can also be applied to screen for glutathione conjugates of reactive metabolites [168].

### 1.6.5

#### Protein Molecular Weight Determination

One of the great benefits of ESI-MS is the ability to generate multiple-charge ions for biomacromolecules such as peptides and proteins, oligonucleotides, and oligosaccharides [169]. In proteins, the multiple charging is due to protonation at the basic amino acids, that is, Lys, His, and Arg, as well as at the N-terminal [170]. On the basis of the  $m/z$  values of the ions in the ion envelope of multiple-charge ions, the molecular weight can be calculated using an averaging algorithm [169, 171]. The algorithm assigns the number of charges to the peaks in the ion envelope and then averages the calculated values for the molecular weight. This simple and straightforward approach can be applied manually to relatively simple spectra with good S/N. Computer algorithms for the deconvolution or transformation of ESI-MS mass spectra of proteins have been developed [171] (see Figure 1.3). An even more powerful software tool is based on maximum-entropy algorithms for transformation of ESI-MS mass spectra [172]. The latter provides far better resolution in the transformed spectrum, enabling detection of small mass differences between proteins in mixtures. These software tools are commercially available from various instrument manufacturers. The maximum-entropy-based

algorithms are especially important if ESI spectra of heterogeneous proteins, for example, glycosylated proteins, are to be transformed.

The deconvolution of ESI spectra of oligonucleotides follows the same lines, except that in the negative-ion ESI mode, deprotonation has to be considered. The deconvolution may be hampered by the presence of  $H^+/Na^+$ -exchange ions in the ion envelope. Therefore, attention has to be paid to adequate desalting of the samples before molecular weight determination [173].

### 1.6.6

#### Peptide Fragmentation and Sequencing

MS using either ESI or MALDI as an ionization technique plays an important role in the characterization of proteins. Next to molecular weight determination of the intact protein (see Section 1.6.5), MS readily enables amino acid sequencing of peptides and proteins (see also Section 1.6.7). On fragmentation in MS–MS, using CID or any of the other ion dissociation techniques, a peptide shows primarily backbone fragmentation. Nomenclature rules have been proposed to readily annotate the spectra [79]. The N-terminal fragments are annotated with *a*, *b*, or *c*, depending on the position of the backbone cleavage (see Figure 1.10), whereas the corresponding C-terminal fragments are annotated with *x*, *y*, and *z*. Under high-energy CID conditions, amino acid side-chain cleavages may occur, leading to *d*, *v*, and *w* ions. Although initially accents were used to indicate protonation and hydrogen rearrangements, for example, the *c* and *y* ions in positive-ion mode were annotated as *c'* and *y'* to indicate that the *y*-ion was generated after rearrangement of a hydrogen to a shorter peptide and subsequent protonation; these accents are nowadays left out in most cases. In low-energy CID, but also in, for instance, SORI and IRMPD, fragmentation occurs at the peptide bond. Thus, predominantly *b* and *y* ions are observed, together with some *a* ions due to CO losses from *b* ions. In peptide sequencing by MS–MS, mostly double-charge ions are

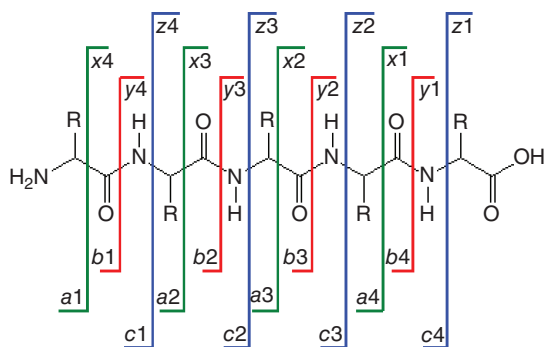


**Figure 1.10** Nomenclature for backbone cleavages of peptides, according to Roepstorff [79]. The N-terminal fragments are annotated with *a*, *b*, or *c*, depending on the

position of the backbone cleavage, whereas the corresponding C-terminal fragments are annotated with *x*, *y*, and *z*.

selected as precursor ions. In that case, next to  $b$  ions both single-charge and double-charge  $y$  ions may be observed. This leads to a series of sequence ions. In ECD and ETD, cleavage of the N–C $_{\alpha}$  bond is observed, thus resulting in even-electron  $c'$  ions and odd-electron  $z\bullet$  ions [75].

For a known amino acid sequence, the  $m/z$  values of the fragment or sequence ions can be easily predicted. To this end, residue masses of amino acids are used, defined as the mass of the amino acid minus water (H $_2$ O, 18.011 Da). The  $m/z$  of the  $b_1$  ion equals 1.007 u (H $^+$ ) plus the residue mass of the N-terminal amino acid; the  $m/z$  of the  $b_2$  ion is that of the  $b_1$  ion plus the residue mass of the second N-terminal amino acid, and so on. The  $m/z$  of the  $y_1$  ion equals 19.018 u (H $_3$ O $^+$ ) plus the residue mass of the C-terminal amino acid; the  $m/z$  of the  $y_2$  ion is that of the  $y_1$  ion plus the residue mass of the second C-terminal amino acid, and so on. Interpretation of the product ion spectrum of a peptide thus involves identifying the series of  $b$  ions and  $y$  ions and fitting the amino acid residue masses in between adjacent peaks. As an example, the annotated product ion spectrum of [Glu1]-fibrinopeptide B is shown in Figure 1.11.

### 1.6.7

#### General Proteomics Strategies: Top-Down, Middle-Down, Bottom-Up

Proteomics involves the large-scale study of structure and functions of the proteins in the complete proteome of an organism or system. MS plays an important role in proteomics studies. In this respect, a proteomics study may be considered as a combination of two workflows, that is, an experimental workflow based on MS and MS–MS analysis of the proteome, and a bioinformatics workflow to efficiently interpret the data acquired. For clarity, these two workflows are best explained for a single protein and its identification first.

In the MS-based experimental workflow, there are three approaches to identify a protein in a proteome, that is, top-down, bottom-up, and middle-down [60, 61].

In the top-down approach, the intact protein, mostly a selected multiple-charge ion generated by ESI as the precursor ion, is subjected to an ion dissociation technique in an MS–MS experiment [60, 61]. High-sensitivity HRMS is needed, preferably using FT-ICR-MS or orbitrap MS systems, as interpretation of the data requires differentiation between the many different charge states that might be present in the product ion spectrum. Significant progress has been made in top-down proteomics [174, 175]. The isolation of the relevant proteins from a proteome is one of the challenges in top-down proteomics as, due to the low diffusion coefficient of proteins, the chromatographic separation of proteins is not very efficient; mostly C $_4$  rather than C $_{18}$  reversed-phase LC is used. Electrophoretic techniques, especially solution-phase isoelectric focusing, can be a powerful alternative. Isolation of individual proteins from complex mixtures by immunoaffinity techniques may be applied. Although CID may be used, the most prominent ion dissociation techniques for top-down proteomics are ECD (with FT-ICR-MS) and ETD (with orbitrap and Q–TOF instruments). In some cases, the internal energy of the selected precursor ion is first increased by CID or infrared laser

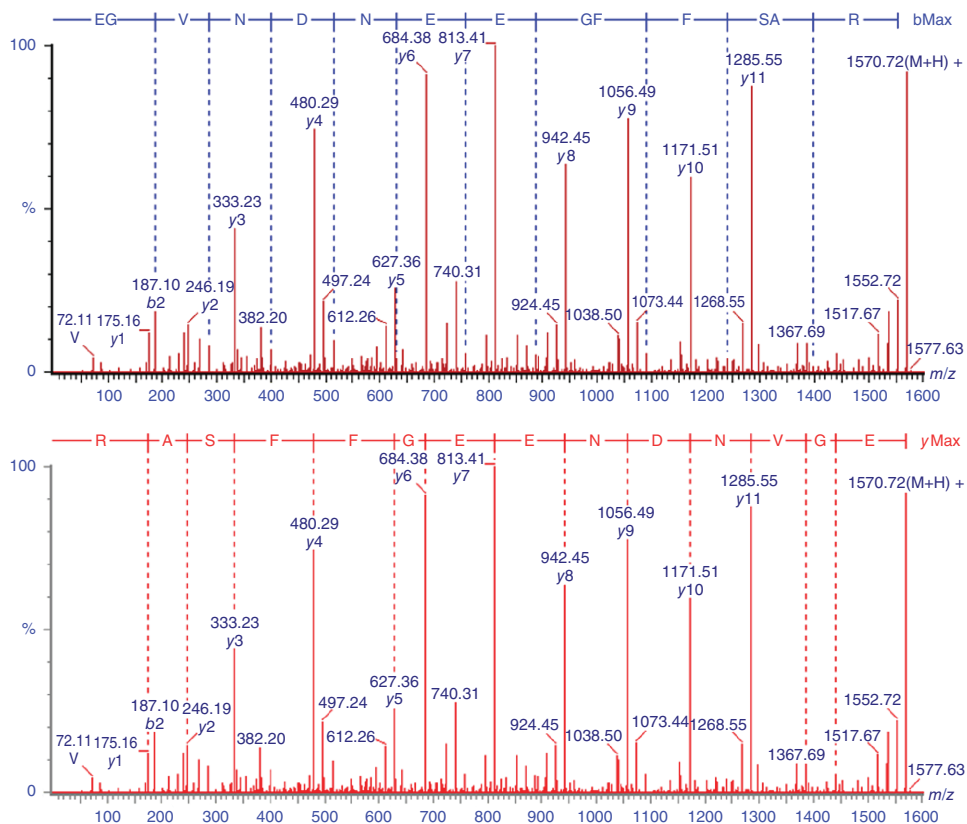


**Figure 1.11** Annotated MS–MS spectrum of the [Glu1]-fibrinopeptide (amino acid sequence: EGVNDNEEGFFSAR), acquired on a Waters Q–TOF 2 instrument and processed using Waters

BioLynx<sup>®</sup> software, part of the Mass-Lynx suite. In the top spectrum the *b*-series are annotated, the bottom one the *y*-series.

light before ECD or ETD. Advanced software tools have been developed for the interpretation of the data [174, 175]. Along these lines, top-down proteomics has been applied for the characterization of intact proteins, especially in mapping posttranslational modifications such as phosphorylation and glycosylation [176], of the study of protein conformations and of noncovalent protein–ligand and protein–protein complexes, where among other techniques H/D-exchange experiments play an important role [177]. Top-down proteomics is expected to play an increasingly important role in the characterization of therapeutic proteins (biopharmaceuticals). Besides ESI-MS approaches, MALDI-TOF-MS has also been applied in top-down proteomics, either by in-source decay [178] or by TOF–TOF approaches [179]. MALDI-FT-ICR-MS may be considered as well.

In the bottom-up approach to protein identification, the intact protein is first enzymatically digested into smaller peptides, after reduction of the Cys–Cys

bridges by dithiothreitol and alkylation of the thiol groups of Cys by iodoacetamide [61, 180]. Peptides can be separated more efficiently using reverse-phase liquid chromatography (RPLC) and can be efficiently fragmented by CID in a wide range of MS–MS instruments. Trypsin is the most widely applied protease for protein digestion [181]. Trypsin cleaves the protein at the C-terminal side of the basic amino acids Arg or Lys, except when there is Pro. This results in peptides (the peptide map or peptide-map fingerprint) that readily form double-charge ions in ESI-MS, which can be selected as precursor ions for efficient CID in MS–MS. The tryptic peptides of an isolated protein or a complete proteome can be separated by RPLC before ESI-MS analysis with DDA to obtain both MS and MS–MS (or MS<sup>n</sup>) data within the same chromatographic run. In the analysis of complex proteomes, on-line two-dimensional (nano-)LC can be used [23, 24]. In this case, the (complex) peptide mixture is fractionated by cation-exchange chromatography by means of a step salt gradient. Each fraction is desalted and preconcentrated on a short RPLC trapping column. The peptide mixture in each fraction is eluted from the trapping column by a solvent gradient (typically consisting of water, acetonitrile, and an acid) onto a (nano-)LC column for peptide separation and on-line ESI-MS analysis with DDA. Powerful software tools have been developed for data processing and interpretation [180].

Data interpretation by the (parallel) bioinformatics workflow can be readily explained for the bottom-up approach [182] (cf. Table 1.2). The starting point of the bioinformatics workflow is the availability of protein databases, eventually derived from DNA or genomic databases. Given the known protease selectivity of trypsin, as well as that of many other proteases, the *in silico* digestion of all proteins in the protein database results in a huge collection of peptides. For each peptide from the *in silico* digestion of the protein database, its mass or *m/z* value, amino acid sequence, and protein ID are stored. MALDI-TOF-MS or LC–MS

**Table 1.2** Bioinformatics workflow complements the parallel biochemical workflow to achieve protein identification based on peptide map.

Experimental workflow	Bioinformatics tools
Isolate the proteome of relevant biological system	(cDNA-derived) Protein sequence database for relevant species
Perform tryptic digestion into complex peptide mixture	Perform <i>in silico</i> digestion of protein database
	List calculated mass of peptides with three pieces of information
	<ul style="list-style-type: none"> <li>• Peptide mass</li> <li>• Amino acid sequence of peptide</li> <li>• Protein ID origin of peptide</li> </ul>
Obtain peptide-mass fingerprint using MALDI-MS or LC–MS	Search experimental masses against calculated masses
List of peptide-masses	Scoring algorithm for possible hits (protein IDs)

analysis of the mixture of tryptic peptides results in a list of  $m/z$  values, the so-called peptide-mass fingerprint or peptide map. This list of  $m/z$  values can be scored against the  $m/z$  values of the peptides from the *in silico* digestion of the protein database. Bioinformatics software tools have been developed to perform this process. In most cases, the scoring algorithm converges to a particular protein from the database, which means that a number of peptides in the peptide map correspond to partial sequences of a particular protein in the database. The software actually provides scoring values on the likeliness that a particular experimental peptide map is derived from a particular protein. In this way, the peptide map may lead to protein identification [183, 184]. When HRMS data can be used, a surprisingly small number of peptides is needed to achieve protein identification.

An alternative workflow involves separation of proteins by one- or two-dimensional gel electrophoresis and staining to visualize the proteins. Spots of interest, for example, specific protein spots or up- or downregulated proteins in a comparative study, can be cut out of the gel. After destaining, in-gel trypsin digestion can be performed. The formed peptides can be readily extracted from the gel and analyzed by either MALDI-TOF-MS or LC-MS to obtain the peptide map or peptide-mass fingerprint, which can be interpreted by means of a similar bioinformatics workflow [185, 186].

**Table 1.3** Bioinformatics workflow complements the parallel biochemical workflow to achieve protein identification based on peptide map and MS<sup>n</sup> information.

Experimental workflow	Bioinformatics tools
Isolate the proteome	Protein sequence database
Perform tryptic digestion	Perform <i>in silico</i> digestion
Obtain peptide-mass fingerprint	Search against calculated masses
List of peptide-masses	Short list of peptides
Acquire MS-MS spectra of peptides in 2D-LC-MS <sup>n</sup>	Predict sequence ions for selected peptides
	Each entry contains:
	<ul style="list-style-type: none"> <li>• Peptide mass (Precursor <math>m/z</math> in MS-MS)</li> <li>• Amino acid sequence of peptide</li> <li>• Predicted sequence ions (<i>b</i> and <i>y</i> ions)</li> <li>• Protein ID origin of peptide</li> </ul>
Data-dependent acquisition in (2D-)-LC-MS <sup>n</sup> results in:	Predict sequence ions for peptides on short list
<ul style="list-style-type: none"> <li>• List of peptide-masses</li> <li>• MS-MS spectra</li> </ul>	
	Search experimental MS-MS data against predicted sequence ions
	Scoring algorithm for possible hits (protein IDs)

This process can even be made more powerful if additionally experimental MS–MS data are available for the peptides in the peptide map. As outlined in Section 1.6.6, the  $m/z$  values of (possible) sequence ions of a peptide with a known sequence can be readily predicted. Thus, the above-mentioned stored information for each peptide from *in silico* digestion (mass or  $m/z$ , amino acid sequence, and protein ID) can be easily complemented by predicted  $m/z$  values of the sequence ions of each of these peptides (cf. Table 1.3). Thus, the  $m/z$  values for the fragment ions in the experimental product ion spectra of all fragmented peptides can be cross-correlated to the information in the database in order to achieve an even more reliable protein identification [187, 188]. Powerful bioinformatics tools have been developed that are based on these principles, for example, MASCOT [189], SEQUEST [190], and advanced modifications thereof [191].

Finally, the middle-down approach shows resemblances to both bottom-up and top-down strategies. The larger protein is first digested in larger fragments, for instance, using the OmpT protease [192], which selectively cleaves between two basic amino acids. The resulting protein fragments are subjected to common top-down proteomics strategies for identification and/or characterization. The application of all three approaches in the characterization of histone variants has recently been reported [193].

## 1.7

### Conclusion and Perspectives

MS is a powerful tool in qualitative and quantitative analysis of compounds with biological relevance. Currently available analyte ionization techniques, especially ESI and MALDI, provide ionization for a wide variety of biomolecules, from small cellular metabolites up to large biomolecular aggregates. The ions generated in this way may be studied with a wide range of mass analyzers, providing molecular mass or weight information on intact molecules. A plethora of tandem MS instruments, featuring a range of different ion activation and dissociation techniques, enables structure elucidation and sequencing. As such, MS is a powerful tool to study biomolecular interactions at different levels, as readily demonstrated in subsequent chapters of the book.

### References

1. Murray, K.K., Boyd, R.K., Eberlin, M.N., Langley, G.J., Li, L., and Naito, Y. (2013) Definitions of terms relating to mass spectrometry (IUPAC Recommendations 2013). *Pure Appl. Chem.*, **85**, 1515–1609.
2. Price, P. (1991) Standard definitions of terms relating to mass spectrometry. A report from the committee on measurements and standards of the American Society for Mass Spectrometry. *J. Am. Soc. Mass Spectrom.*, **2**, 336–348.
3. Sparkman, O.D. (2000) *Mass Spec Desk Reference*, Global View Publishing, Pittsburgh, PA.
4. Urban, J., Afseth, N.K., and Štys, D. (2014) Fundamental definitions and confusions in mass spectrometry about

- mass assignment, centroiding and resolution. *Trends Anal. Chem.*, **52**, 126–136.
- Brenton, A.G. and Godfrey, A.R. (2010) Accurate mass measurement: terminology and treatment of data. *J. Am. Soc. Mass Spectrom.*, **21**, 1821–1835.
  - Kind, T. and Fiehn, O. (2006) Metabolomic database annotations via query of elemental compositions: mass accuracy is insufficient even at less than 1 ppm. *BMC Bioinf.*, **7**, 234.
  - Kind, T. and Fiehn, O. (2007) Seven golden rules for heuristic filtering of molecular formulas obtained by accurate mass spectrometry. *BMC Bioinf.*, **8**, 105.
  - Pelander, A., Tyrkkö, E., and Ojanperä, I. (2009) In silico methods for predicting metabolism and mass fragmentation applied to quetiapine in liquid chromatography/time-of-flight mass spectrometry urine drug screening. *Rapid Commun. Mass Spectrom.*, **23**, 506–514.
  - Nakabayashi, R., Sawada, Y., Yamada, Y., Suzuki, M., Hirai, M.Y., Sakurai, T., and Saito, K. (2013) Combination of liquid chromatography-Fourier transform ion cyclotron resonance-mass spectrometry with  $^{13}\text{C}$ -labeling for chemical assignment of sulfur-containing metabolites in onion bulbs. *Anal. Chem.*, **85**, 1310–1315.
  - Scigelova, M., Hornshaw, M., Giannokopoulos, A., and Makarov, A. (2011) Fourier transform mass spectrometry. *Mol. Cell. Proteomics*, **10**, M111.009431.1–M111.009431.19.
  - Vestal, M.L. (1983) Ionization techniques for nonvolatile molecules. *Mass Spectrom. Rev.*, **2**, 447–480.
  - Cech, N.B. and Enke, C.G. (2001) Practical implications of some recent studies in electrospray ionization fundamentals. *Mass Spectrom. Rev.*, **20**, 362–387.
  - Gabelica, V. and De Pauw, E. (2005) Internal energy and fragmentation of ions produced in electrospray sources. *Mass Spectrom. Rev.*, **24**, 566–587.
  - Kelly, R.T., Tolmachev, A.V., Page, J.S., Tang, K., and Smith, R.D. (2010) The ion funnel: theory, implementations, and applications. *Mass Spectrom. Rev.*, **29**, 294–312.
  - Giles, K., Pringle, S.D., Worthington, K.R., Little, D., Wildgoose, J.L., and Bateman, R.H. (2004) Applications of a travelling wave-based radio-frequency-only stacked ring ion guide. *Rapid Commun. Mass Spectrom.*, **18**, 2401–2414.
  - Lorenzen, K. and van Duijn, E. (2010) Native mass spectrometry as a tool in structural biology. *Curr. Protoc. Protein Sci.*, **62**, 17.12.1–17.12.17.
  - Kebarle, P. and Peschke, M. (2000) On the mechanisms by which the charged droplets produced by electrospray lead to gas phase ions. *Anal. Chim. Acta*, **406**, 11–35.
  - Smith, R.D. and Light-Wahl, K.J. (1993) The observation of non-covalent interactions in solution by electrospray ionization mass spectrometry: promise, pitfalls and prognosis. *Biol. Mass Spectrom.*, **22**, 493–501.
  - Dole, M., Hines, R.L., Mack, L.L., Mobley, R.C., Ferguson, L.D., and Alice, M.B. (1968) Molecular beams of macroions. *J. Chem. Phys.*, **49**, 2240–2249.
  - Iribarne, J.V. and Thomson, B.A. (1976) On the evaporation of small ions from charged droplets. *J. Chem. Phys.*, **64**, 2287–2294.
  - Fenn, J.B., Mann, M., Meng, C.K., Wong, S.F., and Whitehouse, C.M. (1990) Electrospray ionization – principles and practice. *Mass Spectrom. Rev.*, **9**, 37–70.
  - Wilm, M.S. and Mann, M. (1996) Analytical properties of the nanoelectrospray ion source. *Anal. Chem.*, **68**, 1–8.
  - Wolters, D.A., Washburn, M.P., and Yates, J.R. III, (2001) An automated multidimensional protein identification technology for shotgun proteomics. *Anal. Chem.*, **73**, 5683–5690.
  - Nägele, E., Vollmer, M., and Hörth, P. (2003) Two-dimensional nano-liquid chromatography-mass spectrometry system for applications in proteomics. *J. Chromatogr. A*, **1009**, 197–205.
  - Yin, H., Killeen, K., Brennen, R., Sobek, D., Werlich, M., and van de Goor, T.

- (2005) Microfluidic chip for peptide analysis with an integrated HPLC column, sample enrichment column, and nanoelectrospray tip. *Anal. Chem.*, **77**, 527–533.
26. Tanaka, K., Waki, H., Ido, Y., Akita, S., Yoshida, Y., and Yoshida, T. (1988) Protein and polymer analyses up to  $m/z$  100 000 by laser ionization time-of-flight mass spectrometry. *Rapid Commun. Mass Spectrom.*, **2**, 151–153.
  27. Karas, M. and Hillenkamp, F. (1988) Laser desorption ionization of proteins with molecular masses exceeding 10 000 Daltons. *Anal. Chem.*, **60**, 2299–2301.
  28. Karas, M. (1996) Matrix-assisted laser desorption ionization MS: a progress report. *Biochem. Soc. Trans.*, **24**, 897–900.
  29. Marvin, L.F., Roberts, M.A., and Fay, L.B. (2003) Matrix-assisted laser desorption/ionization time-of-flight mass spectrometry in clinical chemistry. *Clin. Chim. Acta*, **337**, 11–21.
  30. Harvey, D.J. (2012) Analysis of carbohydrates and glycoconjugates by matrix-assisted laser desorption/ionization mass spectrometry: an update for 2007–2008. *Mass Spectrom. Rev.*, **31**, 183–311.
  31. Angel, P.M. and Caprioli, R.M. (2013) Matrix-assisted laser desorption ionization imaging mass spectrometry: in situ molecular mapping. *Biochemistry*, **52**, 3818–3828.
  32. Clark, A.E., Kaleta, E.J., Arora, A., and Wolk, D.M. (2013) Matrix-assisted laser desorption ionization-time of flight mass spectrometry: a fundamental shift in the routine practice of clinical microbiology. *Clin. Microbiol. Rev.*, **26**, 547–603.
  33. Tang, N., Tornatore, P., and Weinberger, S.R. (2004) Current developments in SELDI affinity technology. *Mass Spectrom. Rev.*, **23**, 34–44.
  34. Van Berkel, G.J., Pasilis, S.P., and Ovchinnikova, O. (2008) Established and emerging atmospheric pressure surface sampling/ionization techniques for mass spectrometry. *J. Mass Spectrom.*, **43**, 1161–1180.
  35. Takáts, Z., Wiseman, J.M., and Cooks, R.G. (2005) Ambient mass spectrometry using desorption electrospray ionization (DESI): instrumentation, mechanisms and applications in forensics, chemistry, and biology. *J. Mass Spectrom.*, **40**, 1261–1275.
  36. Wu, C., Dill, A.L., Eberlin, L.S., Cooks, R.G., and Ifa, D.R. (2013) Mass spectrometry imaging under ambient conditions. *Mass Spectrom. Rev.*, **32**, 218–243.
  37. Li, A., Wang, H., Ouyang, Z., and Cooks, R.G. (2011) Paper spray ionization of polar analytes using non-polar solvents. *Chem. Commun.*, **47**, 2811–2813.
  38. Zhang, Y., Ju, Y., Huang, C., and Wysocki, V.H. (2014) Paper spray ionization of noncovalent protein complexes. *Anal. Chem.*, **86**, 1342–1346.
  39. Niessen, W.M.A., Manini, P., and Andreoli, R. (2006) Matrix effects in quantitative pesticide analysis using liquid chromatography-mass spectrometry. *Mass Spectrom. Rev.*, **25**, 881–899.
  40. García, M.C., Hogenboom, A.C., Zappey, H., and Irth, H. (2002) Effect of the mobile phase composition on the separation and detection of intact proteins by reversed-phase liquid chromatography-electrospray mass spectrometry. *J. Chromatogr. A*, **957**, 187–199.
  41. Kostianen, R. and Kauppila, T.J. (2009) Effect of eluent on the ionization process in liquid chromatography-mass spectrometry. *J. Chromatogr. A*, **1216**, 685–699.
  42. Börnsen, K.O., Gass, M.A., Bruin, G.J., von Adrichem, J.H., Biro, M.C., Kresbach, G.M., and Ehrat, M. (1997) Influence of solvents and detergents on matrix-assisted laser desorption/ionization mass spectrometry measurements of proteins and oligonucleotides. *Rapid Commun. Mass Spectrom.*, **11**, 603–609.
  43. Amini, A., Dormady, S.J., Riggs, L., and Regnier, F.E. (2000) The impact of buffers and surfactants from micellar electrokinetic chromatography on

- matrix-assisted laser desorption ionization (MALDI) mass spectrometry of peptides. Effect of buffer type and concentration on mass determination by MALDI-time-of-flight mass spectrometry. *J. Chromatogr. A*, **894**, 345–355.
44. De Hoffmann, E. and Stroobant, V. (2007) *Mass Spectrometry. Principles and Applications*, 3rd edn, John Wiley & Sons, Ltd, Chichester.
  45. Makarov, A., Denisov, E., Kholomeev, A., Balschun, W., Lange, O., Strupat, K., and Horning, S. (2006) Performance evaluation of a hybrid linear ion trap/orbitrap mass spectrometer. *Anal. Chem.*, **78**, 2113–2120.
  46. Miller, P.E. and Denton, M.B. (1986) The quadrupole mass filter: basic operating concepts. *J. Chem. Educ.*, **63**, 617–622.
  47. Hager, J.W. (2002) A new linear ion trap mass spectrometer. *Rapid Commun. Mass Spectrom.*, **16**, 512–526.
  48. Schwartz, J.C., Senko, M.W., and Syka, J.E.P. (2002) A two-dimensional quadrupole ion trap mass spectrometer. *J. Am. Soc. Mass Spectrom.*, **13**, 659–669.
  49. Douglas, D.J., Frank, A.J., and Mao, D. (2005) Linear ion traps in mass spectrometry. *Mass Spectrom. Rev.*, **24**, 1–29.
  50. Jonscher, K.R. and Yates, J.R. III, (1997) The quadrupole ion trap mass spectrometer – a small solution to a big challenge. *Anal. Biochem.*, **244**, 1–15.
  51. March, R.E. (1997) An introduction to quadrupole ion trap mass spectrometry. *J. Mass Spectrom.*, **32**, 351–369.
  52. Olsen, J.V., Schwartz, J.C., Griep-Raming, J., Nielsen, M.L., Damoc, E., Denisov, E., Lange, O., Remes, P., Taylor, D., Splendore, M., Wouters, E.R., Senko, M., Makarov, A., Mann, M., and Horning, S. (2009) A dual pressure linear ion trap Orbitrap instrument with very high sequencing speed. *Mol. Cell. Proteomics*, **8**, 2759–2769.
  53. Guilhaus, M., Selby, D., and Mlynski, V. (2000) Orthogonal acceleration time-of-flight mass spectrometry. *Mass Spectrom. Rev.*, **19**, 65–107.
  54. Lacorte, S. and Fernandez-Alba, A.R. (2006) Time of flight mass spectrometry applied to the liquid chromatographic analysis of pesticides in water and food. *Mass Spectrom. Rev.*, **25**, 866–880.
  55. Vestal, M.L., Juhasz, P., and Martin, S.A. (1995) Delayed extraction matrix-assisted laser desorption time-of-flight mass spectrometry. *Rapid Commun. Mass Spectrom.*, **9**, 1044–1050.
  56. Doroshenko, V.M. and Cotter, R.J. (1989) Ideal velocity focusing in a reflectron time-of-flight mass spectrometer. *J. Am. Soc. Mass Spectrom.*, **10**, 992–999.
  57. Xie, C., Zhong, D., Yu, K., and Chen, X. (2012) Recent advances in metabolite identification and quantitative bioanalysis by LC-Q-TOF MS. *Bioanalysis*, **4**, 937–959.
  58. Marshall, A., Hendrickson, C.L., and Jackson, G.S. (1998) Fourier transform ion cyclotron resonance mass spectrometry: a primer. *Mass Spectrom. Rev.*, **17**, 1–35.
  59. Römpf, A., Taban, I.M., Mihalca, R., Duursma, M.C., Mize, T.H., McDonnel, L.A., and Heeren, R.M. (2005) Examples of Fourier transform ion cyclotron resonance mass spectrometry developments: from ion physics to remote access biochemical mass spectrometry. *Eur. J. Mass Spectrom.*, **11**, 443–456.
  60. Kelleher, N.L., Lin, H.Y., Valaskovic, G.A., Aserud, D.J., Fridriksson, E.K., and McLafferty, F.W. (1999) Top-down versus bottom-up protein characterization by tandem high-resolution mass spectrometry. *J. Am. Chem. Soc.*, **121**, 806–812.
  61. Bogdanov, B. and Smith, R.D. (2005) Proteomics by FTICR mass spectrometry: top down and bottom up. *Mass Spectrom. Rev.*, **24**, 168–200.
  62. Hu, Q., Noll, R.J., Li, H., Makarov, A., Hardman, M., and Cooks, G.R. (2005) The Orbitrap: a new mass spectrometer. *J. Mass Spectrom.*, **40**, 430–443.
  63. Geiger, T., Cox, J., and Mann, M. (2010) Proteomics on an Orbitrap benchtop mass spectrometer using

- all-ion fragmentation. *Mol. Cell. Proteomics*, **9**, 2252–2261.
64. Allen, J.S. (1947) An improved electron multiplier particle counter. *Rev. Sci. Instrum.*, **18**, 739–749.
  65. Wiza, J.L. (1979) Microchannel plate detectors. *Nucl. Instrum. Methods*, **162**, 587–601.
  66. Busch, K.L., Glish, G.L., and McLuckey, S.A. (1988) *Mass Spectrometry—Mass Spectrometry. Techniques and Applications of Tandem Mass Spectrometry*, VCH Publishers, Inc., New York.
  67. Hipple, J.A., Fox, R.E., and Condon, E.U. (1946) Metastable ions formed by electron impact in hydrocarbon gases. *Phys. Rev.*, **69**, 347–356.
  68. Yost, R.A. and Enke, C.G. (1978) Selected ion fragmentation with a tandem quadrupole mass spectrometer. *J. Am. Chem. Soc.*, **100**, 2274–2275.
  69. Louris, J.N., Cooks, R.G., Syka, J.E.P., Kelley, P.E., Stafford, G.C. Jr., and Todd, J.F.J. (1987) Instrumentation, applications, and energy deposition in quadrupole ion-trap tandem mass spectrometry. *Anal. Chem.*, **59**, 1677–1685.
  70. Morris, H.R., Paxton, T., Dell, A., Langhorne, J., Berg, M., Bordoli, R.S., Hoyes, J., and Bateman, R.H. (1996) High-sensitivity collisionally-activated decomposition tandem mass spectrometry on a novel quadrupole–orthogonal acceleration time-of-flight mass spectrometer. *Rapid Commun. Mass Spectrom.*, **10**, 889–896.
  71. Bienvenut, W.V., Déon, C., Pasquarello, C., Campbell, J.M., Sanchez, J.C., Vestal, M.L., and Hochstrasser, D.F. (2002) Matrix-assisted laser desorption/ionization-tandem mass spectrometry with high resolution and sensitivity for identification and characterization of proteins. *Proteomics*, **2**, 868–876.
  72. Johnson, J.V., Yost, R.A., Kelley, P.E., and Bradford, D.C. (1990) Tandem-in-space and tandem-in-time mass spectrometry: triple quadrupoles and quadrupole ion traps. *Anal. Chem.*, **62**, 2162–2172.
  73. Sleno, L. and Volmer, D.A. (2004) Ion activation methods for tandem mass spectrometry. *J. Mass Spectrom.*, **39**, 1091–1112.
  74. Laskin, J. and Futrell, J.H. (2005) Activation of large ions in FT-ICR mass spectrometry. *Mass Spectrom. Rev.*, **24**, 135–167.
  75. Zhurov, K.O., Fornelli, L., Wodrich, M.D., Laskay, Ü.A., and Tsybin, Y.O. (2013) Principles of electron capture and transfer dissociation mass spectrometry applied to peptide and protein structure analysis. *Chem. Soc. Rev.*, **42**, 5014–5030.
  76. Kim, M.-S. and Pandey, A. (2012) Electron transfer dissociation mass spectrometry in proteomics. *Proteomics*, **12**, 530–542.
  77. Wührer, M., Catalina, M.I., Deelder, A.M., and Hokke, C.H. (2007) Glycoproteomics based on tandem mass spectrometry of glycopeptides. *J. Chromatogr. B*, **849**, 115–128.
  78. Zubarev, R.A., Kelleher, N.L., and McLafferty, F.W. (1998) Electron capture dissociation of multiply charged protein cations. A nonergodic process. *J. Am. Chem. Soc.*, **120**, 3265–3266.
  79. Roepstorff, P. and Fohlman, J. (1984) Proposal for a common nomenclature for sequence ions in mass spectra of peptides. *Biomed. Mass Spectrom.*, **11**, 601.
  80. Syka, J.E., Coon, J.J., Schroeder, M.J., Shabanowitz, J., and Hunt, D.F. (2004) Peptide and protein sequence analysis by electron transfer dissociation mass spectrometry. *Proc. Natl. Acad. Sci. U.S.A.*, **101**, 9528–9533.
  81. Mansoori, B.A., Dyer, E.W., Lock, C.M., Bateman, K., Boyd, R.K., and Thomson, B.A. (1998) Analytical performance of a high-pressure radiofrequency-only quadrupole collision cell with a axial field applied by using conical rods. *J. Am. Soc. Mass Spectrom.*, **9**, 775–788.
  82. van Dongen, W.D. and Niessen, W.M.A. (2012) LC-MS systems for quantitative bioanalysis. *Bioanalysis*, **4**, 2391–2399.
  83. Hopfgartner, G. and Bourgoigne, E. (2003) Quantitative high-throughput analysis of drugs in biological matrices by mass spectrometry. *Mass Spectrom. Rev.*, **22**, 195–214.

84. Xu, R.N., Fan, L., Rieser, M.J., and El-Shourbagy, T.A. (2007) Recent advances in high-throughput quantitative bioanalysis by LC-MS/MS. *J. Pharm. Biomed. Anal.*, **44**, 342–355.
85. Jemal, M., Ouyang, Z., and Xia, Y.Q. (2010) Systematic LC-MS/MS bio-analytical method development that incorporates plasma phospholipids risk avoidance, usage of incurred sample and well thought-out chromatography. *Biomed. Chromatogr.*, **24**, 2–19.
86. Cherta, L., Portolés, T., Beltran, J., Pitarch, E., Mol, J.G., and Hernández, F. (2013) Application of gas chromatography-(triple quadrupole) mass spectrometry with atmospheric pressure chemical ionization for the determination of multiclass pesticides in fruits and vegetables. *J. Chromatogr. A*, **1314**, 224–240.
87. Hunt, D.F., Shabanowitz, J., Harvey, T.M., and Coates, M.L. (1983) Analysis of organics in the environment by functional group using a triple quadrupole mass spectrometer. *J. Chromatogr.*, **271**, 93–105.
88. Johnson, J.V. and Yost, R.A. (1985) Tandem mass spectrometry for trace analysis. *Anal. Chem.*, **57**, 758A–768A.
89. Wolfender, J.-L., Rodriguez, S., and Hostettmann, K. (1998) Liquid chromatography coupled to mass spectrometry and nuclear magnetic resonance spectroscopy for the screening of plant constituents. *J. Chromatogr. A*, **794**, 299–316.
90. Kind, T. and Fiehn, O. (2010) Advances in structure elucidation of small molecules using mass spectrometry. *Bioanal. Rev.*, **2**, 23–60.
91. van der Hooft, J.J., Vervoort, J., Bino, R.J., Beekwilder, J., and de Vos, R.C. (2011) Polyphenol identification based on systematic and robust high-resolution accurate mass spectrometry fragmentation. *Anal. Chem.*, **83**, 409–416.
92. Macht, M., Asperger, A., and Deininger, S.O. (2004) Comparison of laser-induced dissociation and high-energy collision-induced dissociation using matrix-assisted laser desorption/ionization tandem time-of-flight (MALDI-TOF/TOF) for peptide and protein identification. *Rapid Commun. Mass Spectrom.*, **18**, 2093–2105.
93. Spengler, B. (1997) Post-source decay analysis in matrix-assisted laser desorption/ionization mass spectrometry of biomolecules. *J. Mass Spectrom.*, **32**, 1019–1036.
94. Cotter, R.J., Griffith, W., and Jelinek, C. (2007) Tandem time-of-flight (TOF/TOF) mass spectrometry and the curved-field reflectron. *J. Chromatogr. B*, **855**, 2–13.
95. Mechref, Y., Novotny, M.V., and Krishnan, C. (2003) Structural characterization of oligosaccharides using MALDI-TOF/TOF tandem mass spectrometry. *Anal. Chem.*, **75**, 4895–4903.
96. Franc, V., Řehulka, P., Raus, M., Stulík, J., Novak, J., Renfrow, M.B., and Šebela, M. (2013) Elucidating heterogeneity of IgA1 hinge-region O-glycosylation by use of MALDI-TOF/TOF mass spectrometry: role of cysteine alkylation during sample processing. *J. Proteomics*, **92**, 299–312.
97. Chernushevich, I.V., Loboda, A.V., and Thomson, B.A. (2001) An introduction to quadrupole–time-of-flight mass spectrometry. *J. Mass Spectrom.*, **36**, 849–865.
98. Campbell, J.L. and Le Blanc, J.C.Y. (2012) Using high-resolution quadrupole TOF technology in DMPK analyses. *Bioanalysis*, **4**, 487–500.
99. Michael, S.M., Chien, B.M., and Lubman, D.M. (1992) An ion trap storage/time-of-flight mass spectrometer. *Rev. Sci. Instrum.*, **63**, 4277–4284.
100. Michael, S.M., Chien, B.M., and Lubman, D.M. (1993) Detection of electrospray ionization using a quadrupole ion trap storage/reflectron time-of-flight mass spectrometer. *Anal. Chem.*, **65**, 2614–2620.
101. Liu, Z.Y. (2012) An introduction to hybrid ion trap/time-of-flight mass spectrometry coupled with liquid chromatography applied to drug metabolism studies. *J. Mass Spectrom.*, **47**, 1627–1642.
102. Giera, M., de Vlieger, J.S.B., Niessen, W.M.A., Lingeman, H., and Irth, H.

- (2010) Structure elucidation of biologically active neomycin N-octyl derivatives in a regioisomeric mixture by means of liquid chromatography – ion trap time-of-flight mass spectrometry. *Rapid Commun. Mass Spectrom.*, **24**, 1439–1446.
103. Hopfgartner, G., Varesio, E., Tschäppät, V., Grivet, C., Bourgogne, E., and Leuthold, L.A. (2004) Triple quadrupole linear ion trap mass spectrometer for the analysis of small molecules and macromolecules. *J. Mass Spectrom.*, **39**, 845–855.
104. Xia, Y.Q., Miller, J.D., Bakhtiar, R., Franklin, R.B., and Liu, D.Q. (2003) Use of a quadrupole linear ion trap mass spectrometer in metabolite identification and bioanalysis. *Rapid Commun. Mass Spectrom.*, **17**, 1137–1145.
105. Patrie, S.M., Charlebois, J.P., Whipple, D., Kelleher, N.L., Hendrickson, C.L., Quinn, J.P., Marshall, A.G., and Mukhopadhyay, B. (2004) Construction of a hybrid quadrupole–Fourier transform ion cyclotron resonance mass spectrometer for versatile MS–MS above 10 kDa. *J. Am. Soc. Mass Spectrom.*, **15**, 1099–1108.
106. Wu, S.L., Jardine, I., Hancock, W.S., and Karger, B.L. (2004) A new and sensitive on-line liquid chromatography/mass spectrometric approach for top-down protein analysis: the comprehensive analysis of human growth hormone in an E. coli lysate using a hybrid linear ion trap/Fourier transform ion cyclotron resonance mass spectrometer. *Rapid Commun. Mass Spectrom.*, **18**, 2201–2207.
107. Syka, J.E., Marto, J.A., Bai, D.L., Horning, S., Senko, M.W., Schwartz, J.C., Ueberheide, B., Garcia, B., Busby, S., Muratore, T., Shabanowitz, J., and Hunt, D.F. (2004) Novel linear quadrupole ion trap/FT mass spectrometer: performance characterization and use in the comparative analysis of histone H3 post-translational modifications. *J. Proteome Res.*, **3**, 621–626.
108. Cheng, X.H., Chen, R.D., Bruce, J.E., Schwartz, B.L., Anderson, G.A., Hofstadler, S.A., Gale, D.C., Smith, R.D., Gao, J.M., Sigal, G.B., Mammen, M., and Whitesides, G.M. (1995) Using ESI-FT-ICR-MS to study competitive binding of inhibitors to carbonic anhydrase. *J. Am. Chem. Soc.*, **117**, 8859–8860.
109. Bruce, J.E., Anderson, G.A., Chen, R., Cheng, X., Gale, D.C., Hofstadler, S.A., Schwartz, B.L., and Smith, R.D. (1995) Bio-affinity characterization mass spectrometry. *Rapid Commun. Mass Spectrom.*, **9**, 644–650.
110. Olsen, J.V., Macek, B., Lange, O., Makarov, A., Horning, S., and Mann, M. (2007) Higher-energy C-trap dissociation for peptide modification analysis. *Nat. Methods*, **4**, 709–712.
111. Michalski, A., Damoc, E., Hauschild, J.P., Lange, O., Wieghaus, A., Makarov, A., Nagaraj, N., Cox, J., Mann, M., and Horning, S. (2011) Mass spectrometry-based proteomics using Q Exactive, a high-performance benchtop quadrupole orbitrap mass spectrometer. *Mol. Cell. Proteomics*, **10**, M111.011015(1-12).
112. Senko, M.W., Remes, P.M., Canterbury, J.D., Mathur, R., Song, Q., Eliuk, S.M., Mullen, C., Earley, L., Hardman, M., Blethrow, J.D., Bui, H., Specht, A., Lange, O., Denisov, E., Makarov, A., Horning, S., and Zabrouskov, V. (2013) Novel parallelized quadrupole/linear ion trap/orbitrap tribrid mass spectrometer improving proteome coverage and Peptide identification rates. *Anal. Chem.*, **85**, 11710–11714.
113. Hill, H.H. Jr., Siems, W.F., St. Louis, R.H., and McMinn, D.G. (1990) Ion mobility spectrometry. *Anal. Chem.*, **62**, 1201A–1209A.
114. Creaser, C.S., Griffiths, J.R., Bramwell, C.J., Noreen, S., Hill, C.A., and Thomas, C.L.P. (2004) Ion mobility spectrometry: a review. Part 1. Structural analysis by mobility measurement. *Analyst*, **129**, 984–994.
115. Huang, Y. and Dodds, E.D. (2013) Ion mobility studies of carbohydrates as group I adducts: isomer specific collisional cross section dependence on metal ion radius. *Anal. Chem.*, **85**, 9728–9735.
116. Valentine, S.J., Counterman, A.E., and Clemmer, D.E. (1999) A database of

- 660 peptide ion cross sections: use of intrinsic size parameters for bona fide predictions of cross sections. *J. Am. Soc. Mass Spectrom.*, **10**, 1188–1211.
117. Wang, B., Valentine, S., Plasencia, M., Raghuraman, S., and Zhang, X. (2010) Artificial neural networks for the prediction of peptide drift time in ion mobility mass spectrometry. *BMC Bioinf.*, **11**, 182.
118. Wyttenbach, T., von Helden, G., and Bowers, M.T. (1996) Gas-phase conformation of biological molecules: bradykinin. *J. Am. Chem. Soc.*, **118**, 8355–8364.
119. Clemmer, D.E. and Jarrold, M.F. (1997) Ion mobility measurements and their applications to clusters and biomolecules. *J. Mass Spectrom.*, **32**, 577–592.
120. Srebalus, C.A., Li, J., Marshall, W.S., and Clemmer, D.E. (1999) Gas-phase separations of electrosprayed peptide libraries. *Anal. Chem.*, **71**, 3918–3927.
121. Kanu, A.B., Dwivedi, P., Tam, M., Matz, L., and Hill, H.H. Jr. (2008) Ion mobility-mass spectrometry. *J. Mass Spectrom.*, **43**, 1–22.
122. Williams, D.M. and Pukala, T.L. (2013) Novel insights into protein misfolding diseases revealed by ion mobility-mass spectrometry. *Mass Spectrom. Rev.*, **32**, 169–187.
123. Wyttenbach, T., Pierson, N.A., Clemmer, D.E., and Bowers, M.T. (2014) Ion mobility analysis of molecular dynamics. *Annu. Rev. Phys. Chem.*, **65**, 175–196.
124. Laphorn, C., Pullen, F., and Chowdhry, B.Z. (2013) Ion mobility spectrometry-mass spectrometry (IMS-MS) of small molecules: separating and assigning structures to ions. *Mass Spectrom. Rev.*, **32**, 43–71.
125. Pringle, S.D., Giles, K., Wildgoose, J.L., Williams, J.P., Slade, S.E., Thalassinou, K., Bateman, R.H., Bowers, M.T., and Scrivens, J.H. (2007) An investigation of the mobility separation of some peptide and protein ions using a new hybrid quadrupole/travelling wave IMS/oa-ToF instrument. *Int. J. Mass Spectrom.*, **261**, 1–12.
126. Olivova, P., Chen, W., Chakraborty, A.B., and Gebler, J.C. (2008) Determination of *N*-glycosylation sites and site heterogeneity in a monoclonal antibody by electrospray quadrupole ion-mobility time-of-flight mass spectrometry. *Rapid Commun. Mass Spectrom.*, **22**, 29–40.
127. Guevremont, R. (2004) High-field asymmetric waveform ion mobility spectrometry: a new tool for mass spectrometry. *J. Chromatogr. A*, **1058**, 3–19.
128. Kolakowski, B.M. and Mester, Z. (2007) Review of applications of high-field asymmetric waveform ion mobility spectrometry (FAIMS) and differential mobility spectrometry (DMS). *Analyst*, **132**, 842–864.
129. Tsai, C.W., Yost, R.A., and Garrett, T.J. (2012) High-field asymmetric waveform ion mobility spectrometry with solvent vapor addition: a potential greener bioanalytical technique. *Bioanalysis*, **4**, 1363–1375.
130. Xia, Y.Q., Wu, S.T., and Jemal, M. (2008) LC-FAIMS-MS/MS for quantification of a peptide in plasma and evaluation of FAIMS global selectivity from plasma components. *Anal. Chem.*, **80**, 7137–7143.
131. Zhong, Y., Hyung, S.J., and Ruotolo, B.T. (2012) Ion mobility-mass spectrometry for structural proteomics. *Expert Rev. Proteomics*, **9**, 47–58.
132. Jurneczko, E. and Barran, P.E. (2011) How useful is ion mobility mass spectrometry for structural biology? The relationship between protein crystal structures and their collision cross sections in the gas phase. *Analyst*, **136**, 20–28.
133. Uetrecht, C., Rose, R.J., van Duijn, E., Lorenzen, K., and Heck, A.J. (2010) Ion mobility mass spectrometry of proteins and protein assemblies. *Chem. Soc. Rev.*, **39**, 1633–1655.
134. Enders, J.R. and McLean, J.A. (2009) Chiral and structural analysis of biomolecules using mass spectrometry and ion mobility-mass spectrometry. *Chirality*, **21**, E253–E264.
135. Stahl, D.C., Swiderek, K.M., Davis, M.T., and Lee, T.D. (1996) Data-controlled automation of liquid

- chromatography/tandem mass spectrometry analysis of peptide mixtures. *J. Am. Soc. Mass Spectrom.*, **7**, 532–540.
136. Wenner, B.R. and Lynn, B.C. (2004) Factors that affect ion trap data-dependent MS/MS in proteomics. *J. Am. Soc. Mass Spectrom.*, **15**, 150–157.
  137. Plumb, R.S., Johnson, K.A., Rainville, P., Smith, B.W., Wilson, I.D., Castro-Perez, J.M., and Nicholson, J.K. (2006) UPLC/MS<sup>E</sup>; a new approach for generating molecular fragment information for biomarker structure elucidation. *Rapid Commun. Mass Spectrom.*, **20**, 1989–1994.
  138. Cho, R., Huang, Y., Schwartz, J.C., Chen, Y., Carlson, T.J., and Ma, J. (2012) MS<sup>M</sup>, an efficient workflow for metabolite identification using hybrid linear ion trap Orbitrap mass spectrometer. *J. Am. Soc. Mass Spectrom.*, **23**, 880–888.
  139. Kostiainen, R., Kotiaho, T., Kuuranne, T., and Auriola, S. (2003) Liquid chromatography/atmospheric pressure ionization-mass spectrometry in drug metabolism studies. *J. Mass Spectrom.*, **38**, 357–372.
  140. Boersema, P.J., Mohammed, S., and Heck, A.J. (2009) Phosphopeptide fragmentation and analysis by mass spectrometry. *J. Mass Spectrom.*, **44**, 861–878.
  141. Commission Decision 2002/657/EC implementing Council Directive 96/23/EC concerning the performance of analytical methods and the interpretation of results. *Off. J. Eur. Commun.*, **L221**, 8–36.
  142. Stolker, A.A.M., Stephany, R.W., and van Ginkel, L.A. (2000) Identification of residues by LC-MS. The application of new EU guidelines. *Analysis*, **28**, 947–951.
  143. Sauvage, F.-L., Gaulier, J.M., Lachâtre, G., and Marquet, P. (2008) Pitfalls and prevention strategies for liquid chromatography-tandem mass spectrometry in the selected reaction-monitoring mode for drug analysis. *Clin. Chem.*, **54**, 1519–1527.
  144. Berendsen, B.J., Stolker, L.A., and Nielen, M.W. (2013) The (un)certainty of selectivity in liquid chromatography tandem mass spectrometry. *J. Am. Soc. Mass Spectrom.*, **24**, 154–163.
  145. Ramanathan, R., Jemal, M., Ramagiri, S., Xia, Y.Q., Humphreys, W.G., Olah, T., and Korfmacher, W.A. (2011) It is time for a paradigm shift in drug discovery bioanalysis: from SRM to HRMS. *J. Mass Spectrom.*, **46**, 595–601.
  146. Little, J.L., Clevon, C.D., and Brown, S.D. (2011) Identification of "known unknowns" utilizing accurate mass data and chemical abstracts service databases. *J. Am. Soc. Mass Spectrom.*, **22**, 348–359.
  147. Thurman, E.M., Ferrer, I., and Fernández-Alba, A.R. (2005) Matching unknown empirical formulas to chemical structure using LC/MS TOF accurate mass and database searching: example of unknown pesticides on tomato skins. *J. Chromatogr. A*, **1067**, 127–134.
  148. Staack, R.F. and Hopfgartner, G. (2007) New analytical strategies in studying drug metabolism. *Anal. Bioanal. Chem.*, **388**, 1365–1380.
  149. Holčapek, M., Kolářová, L., and Nobilis, M. (2008) High-performance liquid chromatography–tandem mass spectrometry in the identification and determination of phase I and phase II drug metabolites. *Anal. Bioanal. Chem.*, **391**, 59–78.
  150. Zhu, M., Zhang, H., and Humphreys, W.G. (2011) Drug metabolite profiling and identification by high-resolution mass spectrometry. *J. Biol. Chem.*, **286**, 25419–25425.
  151. Singh, S., Handa, T., Narayanam, M., Sahu, A., Junwal, M., and Shah, R.P. (2012) A critical review on the use of modern sophisticated hyphenated tools in the characterization of impurities and degradation products. *J. Pharm. Biomed. Anal.*, **69**, 148–173.
  152. Kerns, E.H., Volk, K.J., Hill, S.E., and Lee, M.S. (1995) Profiling new taxanes using LC/MS and LC/MS/MS substructural analysis techniques. *Rapid Commun. Mass Spectrom.*, **9**, 1539–1545.
  153. Kerns, E.H., Rourick, R.A., Volk, K.J., and Lee, M.S. (1997) Buspirone metabolite structure profile using a

- standard liquid chromatographic–mass spectrometric protocol. *J. Chromatogr. B*, **698**, 133–145.
154. Li, A.C., Gohdes, M.A., and Shou, W.Z. (2007) “N-in-one” strategy for metabolite identification using a liquid chromatography/hybrid triple quadrupole linear ion trap instrument using multiple dependent product ion scans triggered with full mass scan. *Rapid Commun. Mass Spectrom.*, **21**, 1421–1430.
155. Li, A.C., Shou, W.Z., Mai, T.T., and Jiang, X.Y. (2007) Complete profiling and characterization of in vitro nefazodone metabolites using two different tandem mass spectrometric platforms. *Rapid Commun. Mass Spectrom.*, **21**, 4001–4008.
156. Zhu, M., Ma, L., Zhang, D., Ray, K., Zhao, W., Humphreys, W.G., Skiles, G., Sanders, M., and Zhang, H. (2006) Detection and characterization of metabolites in biological matrices using mass defect filtering of liquid chromatography/high resolution mass spectrometry data. *Drug Metab. Dispos.*, **34**, 1722–1733.
157. Zhang, H., Zhang, D., Ray, K., and Zhu, M. (2009) Mass defect filter technique and its applications to drug metabolite identification by high-resolution mass spectrometry. *J. Mass Spectrom.*, **44**, 999–1016.
158. Liu, D.Q. and Hop, C.E.C.A. (2005) Strategies for characterization of drug metabolites using liquid chromatography–tandem mass spectrometry in conjunction with chemical derivatization and on-line H/D exchange approaches. *J. Pharm. Biomed. Anal.*, **37**, 1–18.
159. Dear, G.J., Munoz-Muriedas, J., Beaumont, C., Roberts, A., Kirk, J., Williams, J.P., and Campuzano, I. (2010) Sites of metabolic substitution: investigating metabolite structures utilising ion mobility and molecular modelling. *Rapid Commun. Mass Spectrom.*, **24**, 3157–3162.
160. Shimizu, A. and Chiba, M. (2013) Ion mobility spectrometry-mass spectrometry analysis for the site of aromatic hydroxylation. *Drug Metab. Dispos.*, **41**, 1295–1299.
161. Shimizu, A., Ohe, T., and Chiba, M. (2012) A novel method for the determination of the site of glucuronidation by ion mobility spectrometry-mass spectrometry. *Drug Metab. Dispos.*, **40**, 1456–1459.
162. Ma, S. and Zhu, M. (2009) Recent advances in applications of liquid chromatography–tandem mass spectrometry to the analysis of reactive drug metabolites. *Chem. Biol. Interact.*, **179**, 25–37.
163. Dieckhaus, C.M., Fernández-Metzler, C.L., King, R., Krolikowski, P.H., and Baillie, T.A. (2005) Negative ion tandem mass spectrometry for the detection of glutathione conjugates. *Chem. Res. Toxicol.*, **18**, 630–638.
164. Castro-Perez, J., Plumb, R., Liang, L., and Yang, E. (2005) A high-throughput liquid chromatography/tandem mass spectrometry method for screening glutathione conjugates using exact mass neutral loss acquisition. *Rapid Commun. Mass Spectrom.*, **19**, 798–804.
165. Zheng, J., Ma, L., Xin, B., Olah, T., Humphreys, W.G., and Zhu, M. (2007) Screening and identification of GSH-trapped reactive metabolites using hybrid triple quadrupole linear ion trap mass spectrometry. *Chem. Res. Toxicol.*, **20**, 757–766.
166. Yan, Z. and Caldwell, G.W. (2004) Stable-isotope trapping and high-throughput screenings of reactive metabolites using the isotope MS signature. *Anal. Chem.*, **76**, 6835–6847.
167. Rousu, T., Pelkonen, O., and Tolonen, A. (2009) Rapid detection and characterization of reactive drug metabolites in vitro using several isotope-labeled trapping agents and ultra-performance liquid chromatography/time-of-flight mass spectrometry. *Rapid Commun. Mass Spectrom.*, **23**, 843–855.
168. Zhu, M., Ma, L., Zhang, H., and Humphreys, W.G. (2007) Detection and structural characterization of glutathione-trapped reactive metabolites using liquid chromatography-high-resolution mass spectrometry and

- mass defect filtering. *Anal. Chem.*, **79**, 8333–8341.
169. Mann, M., Meng, C.K., and Fenn, J.B. (1989) Interpreting mass spectra of multiply charged ions. *Anal. Chem.*, **61**, 1702–1708.
  170. Smith, R.D., Loo, J.A., Edmonds, C.G., Barinaga, C.J., and Udseth, H.R. (1990) New developments in biochemical mass spectrometry: electrospray ionization. *Anal. Chem.*, **62**, 882–899.
  171. Covey, T.R., Bonner, R.F., Shushan, B.I., and Henion, J.D. (1988) The determination of protein, oligonucleotide and peptide molecular weights by ESI-MS. *Rapid Commun. Mass Spectrom.*, **2**, 249–256.
  172. Ferrige, A.G., Seddon, M.J., Green, B.N., Jarvis, S.A., and Skilling, J. (1992) Disentangling electrospray spectra with maximum entropy. *Rapid Commun. Mass Spectrom.*, **6**, 707–711.
  173. Castleberry, C.M., Rodicio, L.P., and Limbach, P.A. (2008) Electrospray ionization mass spectrometry of oligonucleotides. *Curr. Protoc. Nucleic Acid Chem.*, **10**, 10.2.1–10.2.19.
  174. Cui, W., Rohrs, H.W., and Gross, M.L. (2011) Top-down mass spectrometry: recent developments, applications and perspectives. *Analyst*, **136**, 3854–3864.
  175. Zhou, H., Ning, Z., Starr, A.E., Abu-Farha, M., and Figeys, D. (2012) Advancements in top-down proteomics. *Anal. Chem.*, **84**, 720–734.
  176. Lanucara, F. and Eyers, C.E. (2013) Top-down mass spectrometry for the analysis of combinatorial post-translational modifications. *Mass Spectrom. Rev.*, **32**, 27–42.
  177. Konermann, L., Vahidi, S., and Sowole, M.A. (2014) Mass spectrometry methods for studying structure and dynamics of biological macromolecules. *Anal. Chem.*, **86**, 213–232.
  178. Demeure, K., Quinton, L., Gabelica, V., and De Pauw, E. (2007) Rational selection of the optimum MALDI matrix for top-down proteomics by in-source decay. *Anal. Chem.*, **79**, 8678–8685.
  179. Fagerquist, C.K. and Sultan, O. (2011) Induction and identification of disulfide-intact and disulfide-reduced  $\beta$ -subunit of Shiga toxin 2 from *Escherichia coli* O157:H7 using MALDI-TOF-TOF-MS/MS and top-down proteomics. *Analyst*, **136**, 1739–1746.
  180. Zhang, Y., Fonslow, B.R., Shan, B., Baek, M.C., and Yates, J.R. III, (2013) Protein analysis by shotgun/bottom-up proteomics. *Chem. Rev.*, **113**, 2343–2394.
  181. Switzar, L., Giera, M., and Niessen, W.M.A. (2013) Protein digestion: an overview of the available techniques and recent developments. *J. Proteome Res.*, **12**, 1067–1077.
  182. Yates, J.R. III, (1998) Mass spectrometry and the age of the proteome. *J. Mass Spectrom.*, **33**, 1–19.
  183. Henzel, W.J., Billeci, T.M., Stults, J.T., Wong, S.C., Grimley, C., and Watanabe, C. (1993) Identifying proteins from two-dimensional gels by molecular mass searching of peptide fragments in protein sequence databases. *Proc. Natl. Acad. Sci. U.S.A.*, **90**, 5011–5015.
  184. Mann, M., Højrup, P., and Roepstorff, P. (1993) Use of mass spectrometric molecular weight information to identify proteins in sequence databases. *Biol. Mass Spectrom.*, **22**, 338–345.
  185. Shevchenko, A., Jensen, O.N., Podtelejnikov, A.V., Sagliocco, F., Wilm, M., Vorm, O., Mortensen, P., Shevchenko, A., Boucherie, H., and Mann, M. (1996) Linking genome and proteome by mass spectrometry: large-scale identification of yeast proteins from two dimensional gels. *Proc. Natl. Acad. Sci. U.S.A.*, **93**, 14440–14445.
  186. Gevaert, K. and Vandekerckhove, J. (2000) Protein identification methods in proteomics. *Electrophoresis*, **21**, 1145–1154.
  187. Yates, J.R. III, Eng, J.K., and McCormack, A.L. (1995) Mining genomes: correlating tandem mass spectra of modified and unmodified peptides to sequences in nucleotide databases. *Anal. Chem.*, **67**, 3202–3210.
  188. Liska, A.J. and Shevchenko, A. (2003) Combining mass spectrometry with database interrogation strategies in proteomics. *Trends Anal. Chem.*, **22**, 291–298.

189. Perkins, D.N., Pappin, D.J., Creasy, D.M., and Cottrell, J.S. (1999) Probability-based protein identification by searching sequence databases using mass spectrometry data. *Electrophoresis*, **20**, 3551–3567.
190. Ducret, A., Van Oostveen, I., Eng, J.K., Yates, J.R. III, and Aebersold, R. (1998) High throughput protein characterization by automated reverse-phase chromatography/electrospray tandem mass spectrometry. *Protein Sci.*, **7**, 706–719.
191. Ahrné, E., Müller, M., and Lisacek, F. (2010) Unrestricted identification of modified proteins using MS/MS. *Proteomics*, **10**, 671–686.
192. Wu, C., Tran, J.C., Zamdborg, L., Durbin, K.R., Li, M., Ahlf, D.R., Early, B.P., Thomas, P.M., Sweedler, J.V., and Kelleher, N.L. (2012) A protease for “middle-down” proteomics. *Nat. Methods*, **9**, 822–824.
193. Moradian, A., Kalli, A., Sweredoski, M.J., and Hess, S. (2014) The top-down, middle-down, and bottom-up mass spectrometry approaches for characterization of histone variants and their post-translational modifications. *Proteomics*, **14**, 489–497.